Supersymmetry breaking in two dimensions: The lattice $N=1$ Wess-Zumino model

Matteo Beccaria*
INFN, Sezione di Lecce, and Dipartimento di Fisica dell'Università di Lecce, Via Arnesano, ex Collegio Fiorini, I-73100 Lecce, Italy

Massimo Campostrini†
INFN, Sezione di Pisa, and Dipartimento di Fisica "Enrico Fermi" dell'Università di Pisa, Via Buonarroti 2, I-56125 Pisa, Italy

Alessandra Feo‡
Dipartimento di Fisica, Università di Parma and INFN Gruppo Collegato di Parma, Parco Area delle Scienze, 7/A, 43100 Parma, Italy
(Received 10 February 2004; published 26 May 2004)

We study dynamical supersymmetry breaking by nonperturbative lattice techniques in a class of two-dimensional $N=1$ Wess-Zumino models. We work in the Hamiltonian formalism and analyze the phase diagram by analytical strong-coupling expansions and explicit numerical simulations with Green function Monte Carlo methods.

DOI: 10.1103/PhysRevD.69.095010 PACS number(s): 12.60.Jv, 02.70.Ss

I. INTRODUCTION

Supersymmetry (SUSY) is playing an increasingly relevant and unifying role in high energy physics. From a purely theoretical point of view, SUSY is required for consistency and finiteness in superstring theory; compactification and SUSY breaking mechanisms are then needed in order to produce a low energy four-dimensional effective action with a residual $N=1$ SUSY. This constraint comes from the phenomenological side where the most popular current extensions of the standard model are actually based on SUSY for at least two reasons. First, supersymmetric grand unification theories are quite successful in predicting $SU(3)\times SU(2)\times U(1)$ gauge couplings unification [1], a fact that can be considered as the main phenomenological motivation for SUSY [2]. Moreover, supersymmetric models solve in a natural way the hierarchy problem [3] of matching the electroweak and grand unified theory (GUT) scales without being spoiled by huge radiative corrections to Higgs boson masses.

However, many features of this scenario still need some clarification. Indeed, $N=1$ SUSY is expected to be exact at the GUT scale around 10^{16} GeV, but must be broken in the TeV region in order to account for the asymmetric mass textures that are currently observed. In particular, this will be true if some superpartner with a mass of a few TeV will be observed in the future CERN Large Hadron Collider (LHC) or Linear Collider experiments. In the model independent analysis, the source of breaking is usually parametrized by a complete set of soft terms whose origin remains however rather unexplained.

In several approaches, it is due to some kind of spontaneous breaking of SUSY in a *hidden* sector and communicated to the minimal supersymmetric standard model (MSSM) particles producing the soft terms. As with every dynamical symmetry breaking, nonperturbative techniques must be exploited and the lattice regularization and renormalization program is of course one of the main lines of research. Indeed, the simultaneous introduction of infrared and ultraviolet cutoffs allows for calculations, such as strong-coupling expansions, that are quite complementary to the usual weak-coupling perturbative analysis.

Beside this, when any known analytical treatment fails, lattice models can also be studied by direct simulations that can provide, in principle, accurate numerical measurements.

In this paper, we address the problem of spontaneous supersymmetry breaking (S^3B) in a simple, but interesting, theoretical laboratory that is the class of Wess-Zumino (WZ) two-dimensional models of chiral superfields with no vector multiplets. Preliminary results on this subject can be found in [4]. Related studies of the two dimensional Wess-Zumino model can be found in [5].

Despite their simplicity, these systems are nontrivial because in two dimensions supersymmetry is not strong enough to predict the exact pattern of breaking, a situation that must be compared with the four dimensional case where WZ models are expected to break supersymmetry if and only if they do at tree level.

Unfortunately, as we shall discuss, lattice strong-coupling expansions provide useful insights, but are unable to reliably predict the physics of the continuum theory and one must resort to a numerical analysis.

Since S^3B is closely related to the symmetry properties of the ground state, it appears to be quite reasonable to adopt some kind of Hamiltonian formulation. Moreover, we will see in the following that, if we wish to preserve a SUSY subalgebra, a conserved Hamiltonian is crucial. However, the traditional algorithms for simulation of lattice field theories are based on the Lagrangian formulation [6]. The main reason is the immediate probabilistic interpretation of the partition function, at least for bosonic systems not suffering from a sign or phase problem; this leads to a host of Monte Carlo algorithms, some of which are extremely efficient. Of course, alternatives based on a more direct Hamiltonian formalism do exist [7], but they are certainly less exploited in high

*Electronic address: Matteo.Beccaria@le.infn.it
†Electronic address: Massimo.Campostrini@df.unipi.it
‡Electronic address: feo@fis.unipr.it

energy physics where emphasis is on Lagrangian symmetries, in particular Poincaré invariance.

On the other hand, Hamiltonian methods have been used in supersymmetric discretized light-cone quantization (SDLCQ) [8] and also are widely exploited in nonrelativistic contexts [9] where the properties of the ground state are typically the simplest and first object of investigation. Moreover, these techniques interlace the brute force numerical calculations with analytical or physical insights about the structure of the ground state wave function, a feature that is quite welcome in the study of S^3B where we expect major changes to show up at the phase transition.

Another important feature of our study concerns the fact that fermions, needed in supersymmetric models, are the major source of complications in the current approaches to lattice simulations. In the Lagrangian approach quantum expectation values are computed by summing over histories of the classical fields, following Feynman's ideas. In the case of fermions, these are Grassmann valued *classical* fields that cannot be analyzed by direct numerical methods. The typical solution amounts to integrating them out and studying the resulting nonlocal bosonic model [10]. This can be nontrivial for a generic model, and a recent detailed account of this problem and whether it can formulate successfully supersymmetric theories on the lattice can be found in [11].

Instead, in the Hamiltonian approach, what is relevant is the algebra of the fields and their conjugate momenta. From this point of view, fermions and bosons differ just by the replacement of commutators by anticommutators and also by the structure of the state space, finite dimensional for fermions in finite volume, infinite dimensional in the bosonic case. Apparently, in the Hamiltonian approach, there is much more symmetry in the treatment of fermions and bosons than in the Lagrangian approach.

Looking at the details of the simulation techniques, however, problems arise with Hamiltonian fermions due to the well known hard sign problem [12]. Roughly speaking, fermion exchanges introduce problematic and unavoidable signs that often break in a substantial way the probabilistic interpretation of quantum expectation values required to build a numerical stochastic algorithm. This deep problem is somewhat milder in $1+1$ dimensions where specific equivalences between fermionic and bosonic fields can be established [13,14]. Also, the topology of fermion dynamics is the simplest possible and helps in taming the sign problem. Actually, for several fermion models in $1+1$ dimensions arising in solid state theory, like, e.g., Hubbard-like models, algorithms can be devised with no sign problem and good efficiency as well as scaling properties [15].

The detailed plan of the paper is the following. In Sec. II we present the model and its lattice Hamiltonian. In Sec. III we compute the first nontrivial order of the strong-coupling expansion of the ground state energy. In Sec. IV we discuss the renormalization group trajectories along which a continuum limit can be reached. In Sec. V we describe a Green function Monte Carlo algorithm. Finally, Sec. VI is devoted to present our numerical results.

II. THE $N=1$ WESS-ZUMINO MODEL IN 1+1 DIMENSIONS

A. Definition of the model and patterns of SUSY breaking

Let us consider the most general SUSY algebra in two dimensions. The generators are split into fermionic and bosonic ones. The algebra with N left-handed fermionic generators $\{Q_L^A\}_{A=1,\ldots,N}$ and $\bar{N}$ right-handed fermionic generators $\{Q_R^A\}_{A=1,\ldots,\bar{N}}$ is denoted by $(N,\bar{N})$. The bosonic generators are the components of the two-momentum (P^0,P^1) and a set of central charges T^{AB}. The nontrivial part of the algebra is

$$\{Q_L^A,Q_L^B\}=\delta^{AB}(P^0-P^1),$$

$$\{Q_R^A,Q_R^B\}=\delta^{AB}(P^0+P^1),$$

$$\{Q_L^A,Q_R^B\}=T^{AB}.$$

In the left-right symmetric case with $(N,\bar{N})=(1,1)$, we denote

$$Q_{1,2}\equiv Q_R^1\pm Q_L^1, \tag{2.1}$$

and find

$$\{Q_a,Q_b\}=2(H\mathbf{1}+P\sigma^1+T\sigma^3)_{ab}, \tag{2.2}$$

where σ^i are the Pauli matrices, $(P^0,P^1)\equiv(H,P)$ and $T\equiv T^{11}$. The minimal realization of this algebra requires a single real chiral multiplet with a real scalar component φ and a Majorana fermion with components $\psi^{1,2}$. The explicit form of the supercharges is

$$Q_{1,2}=\int dx\left[p(x)\psi^{1,2}(x)-\left(\frac{\partial\varphi}{\partial x}\pm V[\varphi(x)]\right)\psi^{2,1}(x)\right], \tag{2.3}$$

where $p(x)$ is the momentum operator conjugate to $\varphi(x)$. The central charge corresponds to a topological quantum number [16]

$$T=\int dx\frac{\partial\varphi}{\partial x}V(\varphi). \tag{2.4}$$

As usual with supersymmetric models, the structure of the Hamiltonian H guarantees that the energy eigenstates have $E\geqslant 0$ because

$$H=\frac{1}{2}(Q_1^2+Q_2^2). \tag{2.5}$$

Invariant states annihilated by both Q_i coincide with the zero energy states and are thus supersymmetric ground states; they must lie in the topologically trivial sector.

The problem of predicting the pattern of S^3B is not easy. In principle, the form of $V(\varphi)$ is enough to determine whether supersymmetry is broken or not. At least at tree level, one easily proves that supersymmetry is broken if and only if V has no zeros. In two dimensions, however, this

conclusion is generally false due to radiative corrections. An analytic nonperturbative tool that can help in the analysis is the Witten index defined as [23]

$$I = \mathrm{Tr}(-1)^F, \tag{2.6}$$

where F is the fermion number. Since supersymmetry is not explicitly broken, contributions from positive-energy bosonic and fermionic states cancel and

$$I = n^B_{E=0} - n^F_{E=0}. \tag{2.7}$$

In finite volume, I is invariant under changes in $V(\varphi)$ that do not modify its asymptotic behavior. In particular, it can be computed at weak coupling where each zero of $V(\varphi)$ is associated to a perturbative zero energy state. Thus, if $V(\varphi)$ has an odd number of zeros, we find $I \neq 0$ and supersymmetry is unbroken. If, on the other hand, $V(\varphi)$ has an even number of zeros, the associated perturbative vacua can contribute I with opposite signs and, when $I=0$, we cannot say anything. In particular, a nontrivial set of perturbative zero energy states with $I=0$ can receive instanton corrections due to tunneling lifting them to positive energies breaking supersymmetry while leaving $I=0$. In such cases, the behavior of the tunneling rate with increasing volume is crucial in answering the question of breaking.

An interesting example of this complicated scenario is discussed in Appendix A of Ref. [23]. We quickly review the analysis since it will be important in the interpretation of our results. When $V(\varphi)=\lambda(\varphi^2+a^2)$, the action of the WZ model is

$$S = \int d^2x \left(\frac{1}{2}(\partial\varphi)^2 + \frac{i}{2}\bar{\psi}\gamma\cdot\partial\psi - \frac{1}{2}\lambda^2(\varphi^2+a^2)^2 - \frac{1}{2}\lambda\varphi\bar{\psi}\psi \right). \tag{2.8}$$

For large positive a^2 the index is zero because there are no zero-energy states. Due to a special conjugation symmetry valid for this model in finite volume, the pattern of breaking is invariant under $a^2 \to -a^2$. This means that for negative a^2, the two zeros of V are bosonic and fermionic and (finite volume) tunneling lifts their energy to a positive value. However, in infinite volume and large negative a^2, the narrow minimum of the potential is protected from radiative corrections and generates an expectation value $\langle\varphi\rangle \neq 0$ signaling the SSB of the Z_2 symmetry $\varphi \to -\varphi$, $\psi \to \gamma_5\psi$. The fermion becomes massive and supersymmetry must be unbroken due to the absence of a massless Goldstino.

The above discussion illustrates that an alternative nonperturbative analysis of the models with $I=0$ is certainly welcome. In the following, we shall put the model on a space-time lattice in order to exploit explicit numerical simulations as well as analytical strong-coupling expansions.

B. Lattice version of the model

On the lattice it is impossible to maintain the full SUSY algebra and it is important to understand what can be said by looking at subalgebras. If we consider one supercharge only, for instance Q_1, and find a state with $Q_1|s\rangle = 0$, we cannot say that it is a zero energy state unless we know that it is in the $T=0$ sector. On the other hand, if no states with $Q_1|s\rangle = 0$ are found in any topological sector, then supersymmetry is certainly broken.

Thus, even if we forget Q_2, we can choose as a clear-cut signal of supersymmetry dynamically breaking the lowest eigenvalue of the operator Q_1^2: if it is positive, we have breaking.

The SUSY algebra (2.2) involves explicitly the generators of space and time infinitesimal translations and is spoiled on the lattice. In the Lagrangian approach, both space and time are discrete and SUSY is completely broken. In the Hamiltonian formulation, time remains continuous and the $D=2$ algebra is reduced to $D=1$ and not totally lost. The full two-dimensional algebra as well as Lorentz invariance are expected to be recovered in the continuum limit.

A lattice version of the above model has been previously studied in Refs. [17,18]. A similar approach to Wess-Zumino models with $N=2$ supersymmetry is discussed in Ref. [19], and numerical investigations are reported in Ref. [20]. On each site of a spatial lattice with L sites, we define a real scalar field φ_n together with its conjugate momentum p_n such that $[p_n, \varphi_m] = -i\delta_{n,m}$. The associated fermion is a Majorana fermion $\psi_{a,n}$ with $a=1,2$ and $\{\psi_{a,n}, \psi_{b,m}\} = \delta_{a,b}\delta_{n,m}$, $\psi^\dagger_{a,n} = \psi_{a,n}$. The fermionic charge

$$Q = \sum_{n=1}^{L} \left[p_n\psi_{1,n} - \left(\frac{\varphi_{n+1}-\varphi_{n-1}}{2} + V(\varphi_n) \right) \psi_{2,n} \right],$$

with arbitrary real function $V(\varphi)$ (called *prepotential* in the following) can be used to define a semipositive definite lattice Hamiltonian

$$H = Q^2. \tag{2.9}$$

This Hamiltonian includes the central charge contribution in the form of a term

$$\sum_n V(\varphi_n)\frac{\varphi_{n+1}-\varphi_{n-1}}{2}, \tag{2.10}$$

that is precisely a discretization of T. Eigenstates of H are divided into invariant Q-singlets with zero energy and Q-doublets with degenerate positive energy. H describes an interacting model, symmetric with respect to Q and this symmetry is respected by the spectrum if and only if the ground state energy is positive. We stress again that Q symmetry breaking implies breaking of the full 2 dimensional supersymmetry, whereas Q symmetry does not imply (in a generic topological sector) 2D SUSY.

We remind that, on the lattice, spontaneous supersymmetry breaking can occur even for finite lattice size L, because tunneling among degenerate vacua connected by Q is forbidden by fermion number conservation.

To write H in a more familiar form, we follow Ref. [18] and replace the two Majorana fermion operators with a single Dirac operator χ satisfying canonical anticommutation rules, i.e., $\{\chi_n, \chi_m\} = 0$, $\{\chi_n, \chi^\dagger_m\} = \delta_{n,m}$:

$$\psi_{1,n}=\frac{(-1)^n-i}{2i^n}(\chi_n^\dagger+i\chi_n),$$

$$\psi_{2,n}=\frac{(-1)^n+i}{2i^n}(\chi_n^\dagger-i\chi_n). \tag{2.11}$$

The Hamiltonian takes then the form

$$\begin{aligned}H&=H_B(p,\varphi)+H_F(\chi,\chi^\dagger,\varphi)\\&=\sum_n\left\{\frac{1}{2}p_n^2+\frac{1}{2}\left(\frac{\varphi_{n+1}-\varphi_{n-1}}{2}+V(\varphi_n)\right)^2\right.\\&\left.-\frac{1}{2}(\chi_n^\dagger\chi_{n+1}+\text{H.c.})+(-1)^nV'(\varphi_n)\left(\chi_n^\dagger\chi_n-\frac{1}{2}\right)\right\}\end{aligned} \tag{2.12}$$

and describes canonical bosonic and fermionic fields with standard kinetic energies and a Yukawa coupling.

This Hamiltonian conserves the total fermion number

$$N_f=\sum_n\chi_n^\dagger\chi_n, \tag{2.13}$$

and can be examined in each sector with definite N_f separately. For reasons that will be understood later, we shall also consider open boundary conditions and restrict the lattice size L to be even. These are constraints that do not affect the physics of the model in the continuum, but will be very welcome by the algorithm we are going to apply.

The simplest way to analyze the pattern of supersymmetry breaking for a given $V(\varphi)$ is to compute the ground state energy E_0. As we mentioned, on the lattice, we can perform such a computation in a nonperturbative way by strong coupling or numerical simulations. However, before discussing these items, we want to stress some identities that can be used together with E_0 to get information on the symmetry of the ground state.

C. Lattice Ward identities

If the vacuum $|0\rangle$ is supersymmetric, $Q|0\rangle=0$ and for each operator X we have

$$\langle 0|\{Q,X\}|0\rangle=0. \tag{2.14}$$

In particular, taking

$$X=\sum_n F(\varphi_n)\psi_{2,n}, \tag{2.15}$$

we obtain

$$\langle 0|\sum_n\left\{F(\varphi_n)\left[\frac{\varphi_{n+1}-\varphi_{n-1}}{2}+V(\varphi_n)\right]+F'(\varphi_n)(-1)^n(\chi_n^\dagger\chi_n-1/2)\right\}|0\rangle=0. \tag{2.16}$$

A basis of Ward identities is thus obtained by considering $F(\varphi)=\varphi^n$. For instance, on an even lattice with open boundary conditions we find for $n=1$ the relation

$$\langle 0|\sum_n\{\varphi_nV(\varphi_n)+(-1)^n\chi_n^\dagger\chi_n\}|0\rangle=0. \tag{2.17}$$

The case $F(\varphi)=$constant is also interesting. It leads to

$$\langle 0|\sum_n V(\varphi_n)|0\rangle=0. \tag{2.18}$$

III. STRONG COUPLING ANALYSIS OF SUSY BREAKING

Let us start from the supersymmetry charge

$$Q=\sum_l\left[p_l\psi_l^1-V(\varphi_l)\psi_l^2-\frac{\varphi_{l+1}-\varphi_{l-1}}{2}\psi_l^2\right].$$

Following Ref. [19], we define the strong-coupling limit by

$$V(\varphi)\to_{\lambda\to\infty}\lambda V^{(0)}(\lambda\varphi),$$

perform the canonical transformation

$$\varphi^{(0)}=\lambda\varphi,\quad p^{(0)}=\frac{1}{\lambda}p,$$

and rescale the energies by λ^2; dropping the index $^{(0)}$ from φ and p, the result is

$$Q=\sum_l\left[p_l\psi_l^1-V(\varphi_l)\psi_l^2-\frac{(\varphi_{l+1}-\varphi_{l-1})\psi_l^2}{2\lambda^2}\right]\equiv Q^{(0)}+\frac{Q^{(2)}}{\lambda^2},$$

$$H=Q^2=\frac{1}{2}\sum_l\left[p_l^2+V^2(\varphi_l)+2iV'(\varphi_l)\psi_l^1\psi_l^2+\frac{(\varphi_{l+1}-\varphi_{l-1})V(\varphi_l)+i\psi_{l+1}^1\psi_l^2+i\psi_{l+1}^2\psi_l^1}{\lambda^2}+\frac{(\varphi_{l+1}-\varphi_{l-1})^2}{4\lambda^4}\right]$$

$$\equiv H^{(0)}+\frac{H^{(2)}}{\lambda^2}+\frac{H^{(4)}}{\lambda^4}.$$

Introducing the Dirac fields χ_l, $\chi_l^\dagger$ [18], cf. Eq. (2.11), we obtain

$$H^{(0)}=\sum_l \left[\frac{1}{2}p_l^2+\frac{1}{2}V^2(\varphi_l)+(-1)^l V'(\varphi_l)(\chi_l^\dagger\chi_l-1/2)\right]=\sum_l \left[\frac{1}{2}p_l^2+\frac{1}{2}V^2(\varphi_l)+\frac{1}{2}(-1)^{l+n_l}V'(\varphi_l)\right]$$

$$H^{(2)}=\frac{1}{2}\sum_l V(\varphi_l)(\varphi_{l+1}-\varphi_{l-1})-\frac{1}{2}\sum_l (\chi_l^\dagger\chi_{l+1}+\text{H.c.})$$

$$H^{(4)}=\frac{1}{8}\sum_l (\varphi_{l+1}-\varphi_{l-1})^2$$

where we denote by $n_l=0,1$ the eigenvalue of $\chi_l^\dagger\chi_l$.

A. Leading order

To leading order in $1/\lambda$, the Hamiltonian is factorized in a supersymmetric quantum mechanics for each site; adopting an explicit representation, we can write the one-site Hamiltonian as

$$H=\frac{1}{2}\left[-\frac{d^2}{dx^2}+V^2(x)+\sigma_3 V'(x)\right] \tag{3.1}$$

[in the occupation number representation the basis chosen now is $(n=0,n=1)$ for odd sites and $(n=1,n=0)$ for even sites]. This Hamiltonian has a $N=2$ supersymmetry [21],

$$\{Q_i,Q_j\}=\delta_{ij}H,$$

$$Q_1=\frac{1}{2}[\sigma_1 p+\sigma_2 V(x)],$$

$$Q_2=\frac{1}{2}[\sigma_2 p-\sigma_1 V(x)]. \tag{3.2}$$

The conditions for a supersymmetric ground state $Q_i\psi_0=0$ reduce to

$$\psi_0'(x)=\sigma_3 V(x)\psi_0(x). \tag{3.3}$$

For polynomial V, supersymmetry is unbroken if and only if it is possible to find a normalizable solution to Eq. (3.3), which happens if the degree q of V is odd [21].

We can write the time-independent Schrödinger equation as

$$\psi''+[2E-V^2(x)\mp V'(x)]\psi=0;$$

denoting the eigenfunctions for the two signs by $\psi_m^\pm$ and their energies by $\varepsilon_m^\pm$, we have

$$\psi_m^{\pm\prime\prime}+[2\varepsilon_m^\pm-V^2(x)\mp V'(x)]\psi_m^\pm=0. \tag{3.4}$$

Supersymmetry implies that, for $E\neq 0$, states are paired in boson-fermion doublets.

We remark that this conclusion is in strong disagreement with the continuum (or weak-coupling lattice) analysis where the relevant feature of V is the existence of zeros.

For $q>1$, $\psi_m^\pm(x)$ and $\varepsilon_m^\pm$ cannot be computed exactly (excluding the cases $\varepsilon_0^\pm=0$); it is however easy to compute then numerically to high accuracy, using, e.g., the Numerov method [22]. An example is shown in Fig. 1.

In the following analysis, we shall have to tell between V with odd or even leading power of φ.

1. Odd q

For odd q, we either have $\varepsilon_0^-=0$ or $\varepsilon_0^+=0$; let us assume $\varepsilon_0^-=0$: ψ_0^- is the supersymmetric ground state satisfying Eq. (3.3); all the other states appear in pairs: $\varepsilon_{m+1}^-=\varepsilon_m^+$. Notice that the ground state is bosonic for even sites, fermionic for odd sites (the opposite holds if $\varepsilon_0^+=0$).

A strong argument against supersymmetry breaking is given by the Witten index $I_W\equiv \mathrm{Tr}(-1)^{N_f}$ [23]; in the strong-coupling limit, we clearly have $I_W=\pm 1$; since $I_W\neq 0$ implies unbroken SUSY, and I_W is invariant under regular perturbations (cf. Sec. III A 3), supersymmetry can never be broken for odd q, not even in the $L\to\infty$ limit.

A simple check of this result can be given explicitly when V is linear and is discussed in details in Appendix A.

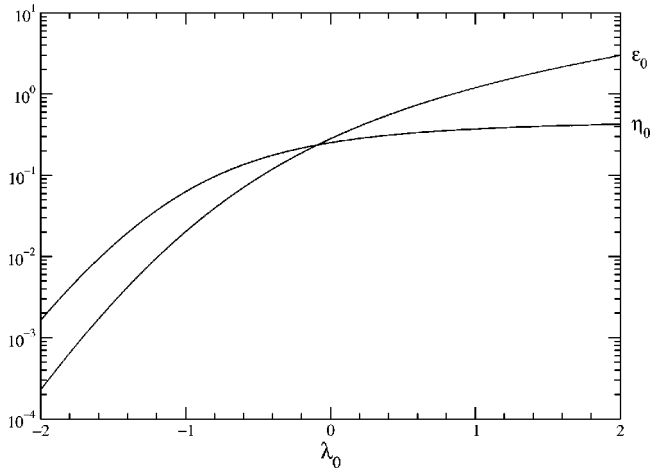

FIG. 1. The ground-state energy $\varepsilon_0=\varepsilon_0^\pm$ and the overlap η_0 as functions of λ_0 for the quadratic prepotential $V=\varphi^2+\lambda_0$.

2. Even q

For even q, we have $\varepsilon_m^+ = \varepsilon_m^-$; for $m=0$, this corresponds to a degenerate ground state with broken supersymmetry ($\varepsilon_0^\pm = \varepsilon_0 > 0$). The phases of the normalized states $|\psi_n^\pm\rangle$ can be chosen in order to satisfy

$$\sqrt{2\varepsilon_n}|\psi_n^-\rangle = [-ip + V(\varphi)]|\psi_n^+\rangle, \tag{3.5}$$

$$\sqrt{2\varepsilon_n}|\psi_n^+\rangle = [ip + V(\varphi)]|\psi_n^-\rangle. \tag{3.6}$$

Introducing the notation

$$\langle \mathcal{O}\rangle_\pm = \langle \psi_0^\pm|\mathcal{O}|\psi_0^\pm\rangle,$$

$$\langle \psi_0^+|\psi_0^-\rangle = \eta_0,$$

we can prove the important relations

$$\langle V\rangle_\pm = \sqrt{2\varepsilon_0}\,\eta_0, \tag{3.7}$$

$$\langle \varphi\rangle_- - \langle \varphi\rangle_+ = \frac{1}{\sqrt{2\varepsilon_0}}\,\eta_0. \tag{3.8}$$

η_0 can be computed numerically from $\psi_0^\pm(\varphi)$, cf. Fig. 1. The proof of Eq. (3.7) is very simple: just take the scalar product of Eq. (3.5) with $\langle \psi_0^+|$ and of Eq. (3.5) with $\langle \psi_0^-|$, and observe that $\langle p\rangle_\pm = 0$. The proof of Eq. (3.8) is also immediate,

$$\begin{aligned}\sqrt{2\varepsilon_0}\langle \psi_0^+|\varphi|\psi_0^+\rangle &= \langle \psi_0^+|\varphi(ip+V)|\psi_0^-\rangle \\ &= \langle \psi_0^+|(ip+V)\varphi|\psi_0^-\rangle + \langle \psi_0^+|i[\varphi,p]|\psi_0^-\rangle \\ &= \sqrt{2\varepsilon_0}\langle \psi_0^-|\varphi|\psi_0^-\rangle - \langle \psi_0^+|\psi_0^-\rangle.\end{aligned}$$

Several simplifications can be exploited when $V(\varphi)$ is even. For an asymptotically positive polynomial $V(\varphi)$ with degree $q \geqslant 2$ it is easy to show that[1]

$$|\psi_n^-\rangle = (-1)^n I|\psi_n^+\rangle$$

where I is the Hermitian parity inversion operator

$$\langle \varphi|I|\psi\rangle = \langle -\varphi|\psi\rangle.$$

Then, the eigenstates can be characterized by the single equation

$$\sqrt{2\varepsilon_n}|\psi_n\rangle = (-1)^n(ip+V)I|\psi_n\rangle$$

where

$$|\psi_n\rangle \equiv |\psi_n^+\rangle.$$

It is easy in this case to obtain generalized relations like the previous ones. Let us consider the equation

$$\begin{aligned}\sqrt{2\varepsilon_n}\langle \psi_m|I|\psi_n\rangle &= (-1)^n\langle \psi_m|I(ip+V)I|\psi_n\rangle \\ &= (-1)^n\langle \psi_m|(-ip+V)|\psi_n\rangle.\end{aligned}$$

Taking the Hermitian conjugate and exchanging m and n we find the two equations

$$\sqrt{2\varepsilon_n}\langle \psi_n|I|\psi_m\rangle = (-1)^n\langle \psi_n|(ip+V)|\psi_m\rangle \tag{3.9}$$

$$\sqrt{2\varepsilon_m}\langle \psi_n|I|\psi_m\rangle = (-1)^m\langle \psi_n|(-ip+V)|\psi_m\rangle \tag{3.10}$$

therefore

$$\langle \psi_n|V(\varphi)|\psi_m\rangle = \frac{1}{\sqrt{2}}[\sqrt{\varepsilon_m}(-1)^m + \sqrt{\varepsilon_n}(-1)^n]\langle \psi_n|I|\psi_m\rangle$$

or (exploiting parity)

$$\langle \psi_n^\pm|V(\varphi)|\psi_m^\pm\rangle = \frac{1}{\sqrt{2}}[\sqrt{\varepsilon_n} + \sqrt{\varepsilon_m}(-1)^{n+m}]\langle \psi_n^\mp|\psi_m^\pm\rangle. \tag{3.11}$$

In a similar way we can compute

$$\sqrt{2\varepsilon_n}\langle \psi_m|\varphi|\psi_n\rangle = (-1)^n\langle \psi_m|\varphi(ip+V)I|\psi_n\rangle.$$

Taking the Hermitian conjugate and exchanging m and n we find the two equations

$$\sqrt{2\varepsilon_n}\langle \psi_n|\varphi|\psi_m\rangle = (-1)^n\langle \psi_n|(-ip-V)\varphi I|\psi_m\rangle \tag{3.12}$$

$$\sqrt{2\varepsilon_m}\langle \psi_n|\varphi|\psi_m\rangle = (-1)^m\langle \psi_n|\varphi(ip+V)I|\psi_m\rangle \tag{3.13}$$

summing the two equations

$$\begin{aligned}&\sqrt{2}[\sqrt{\varepsilon_n}(-1)^n + \sqrt{\varepsilon_m}(-1)^m]\langle \psi_n|\varphi|\psi_m\rangle \\ &\quad = \langle \psi_n i[\varphi,p]I|\psi_m\rangle = -\langle \psi_n|I|\psi_m\rangle\end{aligned}$$

and (exploiting parity)

$$\langle \psi_n^\pm|\varphi|\psi_m^\pm\rangle = \mp\frac{1}{\sqrt{2}}\,\frac{1}{\sqrt{\varepsilon_n} + (-1)^{n+m}\sqrt{\varepsilon_m}}\langle \psi_n^\mp|\psi_m^\pm\rangle. \tag{3.14}$$

Of course, for $n=m=0$, Eqs. (3.11), (3.14) agree with the previous general results.

3. On the convergence of the perturbative expansion

The Rayleigh-Schrödinger perturbation theory of a Hamiltonian of the form $H = H_0 + \beta H_1$ is regular (i.e., it has a finite radius of convergence in β) if [24]

$$\|H_1\Psi\| \leqslant a\|H_0\Psi\| + b\|\Psi\| \tag{3.15}$$

[1]In fact, from their definition, one can see that $\psi_n^\pm(\varphi)$ have the same sign when $\varphi \to +\infty$. Since they are related by a parity transformation, their relative phase is fixed by the number of nodes.

uniformly for all state vectors Ψ; in our case, Eq. (3.15) clearly holds, for both $H^{(2)}$ and $H^{(4)}$, except for the trivial cases $q \leqslant 1$.

B. First order

At first order (subleading) in the strong-coupling expansion we consider again the two cases of even or odd q.

1. Odd q

In the case of unbroken supersymmetry (odd q), the subleading correction to the ground-state energy in the strong-coupling expansion is zero: the fermionic contribution $i\psi^1_{l+1}\psi^2_l + i\psi^2_{l+1}\psi^1_l$ has clearly zero diagonal matrix elements, and the bosonic contribution $\varphi_{l+1}V(\varphi_l) - \varphi_l V(\varphi_{l+1})$ is zero because it factorizes into $\langle\varphi\rangle\langle V\rangle - \langle\varphi\rangle\langle V\rangle$; strictly speaking, this is true for periodic and free boundary conditions, but it could be false, e.g., for fixed boundary conditions.

2. Even q

Due to the structure of the Hamiltonian, it is convenient to describe states in the mixed form

$$\sum_{n_1,\ldots,n_L} \psi_{n_1,\ldots,n_L}(\varphi_1,\ldots,\varphi_L)|n_1,\ldots,n_L\rangle \tag{3.16}$$

where $\psi_{n_1,\ldots,n_L}(\varphi_1,\ldots,\varphi_L)$ is a wave function depending on the bosonic degrees of freedom and $|n_1,\ldots,n_L\rangle$ is the fermionic component of the state defined in terms of the state annihilated by all χ,

$$\chi_i|0\rangle = 0, \tag{3.17}$$

according to the canonical ordering of the Fermi operators:

$$|n_1,\ldots,n_L\rangle = (\chi_1^\dagger)^{n_1}\cdots(\chi_L^\dagger)^{n_L}|0\rangle. \tag{3.18}$$

Of course $n_i = 0,1$ and $|n_1,\ldots,n_L\rangle$ describes a state with n_i fermions at site i. In the case of broken supersymmetry (even q), the subspace $\mathcal{B}$ of lowest leading-order energy is spanned by the states

$$|\boldsymbol{n}\rangle = \psi_0^{\sigma_1}(\varphi_1)\cdots\psi_0^{\sigma_L}(\varphi_L)|n_1,\ldots,n_L\rangle, \tag{3.19}$$

where $\sigma_l = (-1)^{l+n_l}$ and $\psi_0^{\pm 1} \equiv \psi_0^{\pm}$. We have adopted open boundary conditions, corresponding in our notations to setting $\varphi_0 = \varphi_{L+1} = 0$ and $\psi_0^a = \psi_{L+1}^a = 0$ (and therefore $\chi_0 = \chi_{L+1} = 0$).

Since the number of fermions $\Sigma_l n_l$ is conserved, we can impose an additional constraint on $\mathcal{B}$ and define

$$\mathcal{B}_N = \left\{ |\boldsymbol{n}\rangle,\ \sum_l n_l = N \right\}, \quad \mathcal{B} = \mathcal{B}_0 \oplus \ldots \oplus \mathcal{B}_L .$$

We will now prove that, for even L, the ground state is doubly degenerate and lies in the sectors with $N = L/2, L/2-1$.

At first order, we have to diagonalize the operator $H^{(2)}$ over $\mathcal{B}_N$. Let us split

$$H^{(2)} = H_B^{(2)} + H_F^{(2)} \tag{3.20}$$

$$H_B^{(2)} = \frac{1}{2}\sum_{l=1}^{L} V(\varphi_l)(\varphi_{l+1} - \varphi_{l-1}) \tag{3.21}$$

$$H_F^{(2)} = -\frac{1}{2}\sum_{l=1}^{L} (\chi_l^\dagger\chi_{l+1} + \chi_{l+1}^\dagger\chi_l). \tag{3.22}$$

Since

$$\langle \boldsymbol{n}'|H_B^{(2)}|\boldsymbol{n}\rangle = \frac{1}{2}\sqrt{2\varepsilon_0}\,\eta_0\,\delta_{\boldsymbol{n},\boldsymbol{n}'}\sum_l (\langle\varphi_{l+1}\rangle - \langle\varphi_{l-1}\rangle) \tag{3.23}$$

we have

$$\langle \boldsymbol{n}'|H_B^{(2)}|\boldsymbol{n}\rangle = -\frac{1}{4}\eta_0^2\,\delta_{\boldsymbol{n},\boldsymbol{n}'}[(-1)^{n_1} + (-1)^{n_L}] \tag{3.24}$$

where we have exploited

$$\langle\varphi_l\rangle = -(-1)^{l+n_l}\frac{\eta_0}{\sqrt{2\varepsilon_0}}, \tag{3.25}$$

that holds for even V. Since $n = 0,1$ we can use $(-1)^n = 1 - 2n$ and write

$$\langle \boldsymbol{n}'|H_B^{(2)}|\boldsymbol{n}\rangle = \frac{1}{2}\eta_0^2\,\delta_{\boldsymbol{n},\boldsymbol{n}'}(-1 + n_1 + n_L). \tag{3.26}$$

The matrix elements of $H_F^{(2)}$ are

$$\langle \boldsymbol{n}'|H_F^{(2)}|\boldsymbol{n}\rangle = -\frac{1}{2}\eta_0^2 h_{\boldsymbol{n},\boldsymbol{n}'} \tag{3.27}$$

where $h_{\boldsymbol{n},\boldsymbol{n}'} = 1$ if $\boldsymbol{n}$ and $\boldsymbol{n}'$ are connected by $H_F^{(2)}$ (i.e. a hopping of one fermion) and 0 otherwise.

Thus, we can hide the bosonic wave functions and write an effective perturbation acting on purely fermionic states as

$$H_{\text{eff}}^{(2)} = \frac{\eta_0^2}{2}\left(\sum_{i,j=1}^{L}\chi_i^\dagger M_{ij}\chi_j - \mathbf{1}\right) \tag{3.28}$$

where $\mathbf{1}$ is the identity operator and

$$M_{ij} = \begin{cases} -1 & |i-j| = 1 \\ 1 & i = j = 1 \text{ or } L \\ 0 & \text{otherwise.} \end{cases} \tag{3.29}$$

Since $H_{\text{eff}}^{(2)}$ is quadratic, it is convenient to change operator basis. Let $v_i^{(p)}$ be the pth eigenvector of M with eigenvalue $\lambda^{(p)}$,

$$v_n^{(p)} = \sqrt{\frac{2-\delta_{p,L}}{L}}\sin\left[\frac{p\pi}{L}\left(n - \frac{1}{2}\right)\right] \tag{3.30}$$

$$\lambda^{(p)} = -2\cos\frac{p\pi}{L}. \tag{3.31}$$

They define a (real) unitary matrix

$$\sum_{p=1}^{L} v_i^{(p)} v_j^{(p)} = \delta_{ij}, \quad \sum_{i=1}^{L} v_i^{(p)} v_i^{(q)} = \delta_{pq}.$$

We can replace the operators χ_i by the operators a_i defined by

$$\chi_i = \sum_{p=1}^{L} v_i^{(p)} a_p, \quad a_p = \sum_{i=1}^{L} v_i^{(p)} \chi_i$$

with

$$\{a_p, a_q^\dagger\} = \delta_{pq}.$$

The new form of $H_{\rm eff}^{(2)}$ is

$$H_{\rm eff}^{(2)} = \frac{\eta_0^2}{2}\left(\sum_{p=1}^{L} \lambda^{(p)} a_p^\dagger a_p - \mathbf{1} \right). \tag{3.32}$$

The eigenvalues $\lambda^{(1)}, \ldots, \lambda^{(L/2-1)}$ are negative and $\lambda^{(L/2)} = 0$; there are thus two degenerate ground states with $L/2 - 1$ and $L/2$ fermions. This is required by supersymmetry: since $H^{(2)}$ restricted to $\mathcal{B}$ commutes with $Q^{(0)}$, all the states must be paired in doublets with N differing by 1. The ground state with $L/2$ fermions is

$$|\Psi_0^{(1)}\rangle = \psi_0^{\sigma_1}(\varphi_1) \cdots \psi_0^{\sigma_L}(\varphi_L) a_1^\dagger \cdots a_{L/2}^\dagger |0\rangle. \tag{3.33}$$

To conclude, the shift of the ground state energy due to the perturbation is

$$E_1 = \frac{\eta_0^2}{2}\left(-1 - 2\sum_{n=1}^{L/2} \cos\frac{\pi n}{L} \right) = -\frac{\eta_0^2}{2} \cot\frac{\pi}{2L}. \tag{3.34}$$

In the $L \to \infty$ limit we have

$$\frac{E_1}{L} = -\frac{\eta_0^2}{\pi} + \mathcal{O}(1/L). \tag{3.35}$$

In summary, the first order perturbation in the strong-coupling expansion removes the large degeneracy of the ground state and determines a doublet of eigenstates with $L/2-1$ and $L/2$ fermions with minimum energy

$$\frac{E}{L} = \varepsilon_0 - \frac{1}{\lambda^2}\frac{\eta_0^2}{\pi} + \mathcal{O}\left(\frac{1}{\lambda^2 L}, \frac{1}{\lambda^4} \right). \tag{3.36}$$

A similar calculation at first order for $\langle \varphi_k \rangle$ and $\langle \varphi_k \varphi_l \rangle_c$ is discussed in Appendix B. The second-order correction to the ground state energy can also be computed with a reasonable effort and the result is described in Appendix C. However, we remark that the results drawn from the first order corrections are not qualitatively changed.

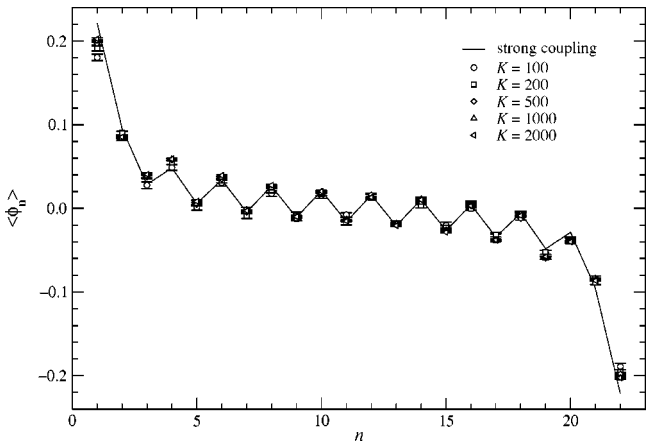

FIG. 2. Comparison between strong coupling and MC simulation for the expectation value $\langle \varphi_n \rangle$ in the quadratic model with $V(\varphi) = 2\varphi^2$ on a lattice with $L = 22$ spatial sites.

C. Discussion

From the analysis of the strong-coupling expansion of the model we can draw the following conclusion. For polynomial $V(\varphi)$, the relevant parameter is just its degree q.

For odd q, the strong coupling analysis and the tree-level results agree and supersymmetry is expected to be unbroken. This conclusion gains further support from the nonvanishing value of the Witten index at strong coupling.

For even q, in strong coupling, the ground state (at least in the sector with half filling) has a positive energy density also for $L \to \infty$ and supersymmetry appears to be broken. Of course, this can be in disagreement with weak coupling. A specific case that we shall analyze numerically in great detail is

$$V(\varphi) = \lambda_2 \varphi^2 + \lambda_0. \tag{3.37}$$

For $\lambda_0 < 0$, weak coupling predicts unbroken SUSY, whereas the strong coupling prediction gives broken SUSY for all λ_0. For this specific model, as we already discussed, the strong coupling analysis agrees with Ref. [23] in the sense that it reproduces the continuum physics in finite volume.

For large expansion parameter, the strong coupling results can be compared with explicit simulations (that we shall fully discuss in Sec. V). Let us consider for instance the quadratic model with $\lambda_0 = 0$ on a lattice with $L = 22$ spatial sites. In Fig. 2, we show the expectation value $\langle \varphi_n \rangle$ computed at $\lambda_2 = 2$. The agreement is quite good apart from the points on the border where the convergence seems to be slower. To check the validity of the strong coupling expansion at smaller couplings, we show in Fig. 3 the ground state energy from MC simulation compared with the first and second order strong coupling expansion. The scaled variables on the plot axes are discussed in Appendix C. The second order gives better results at large values of the expansion parameter, but is unreliable below $\lambda_2 \simeq 0.35$.

In the next section, we shall see that the continuum limit is in the region of small λ_2. Thus, for even q, it seems difficult to gain additional insight from strong coupling and some kind of transition can happen as the continuum limit is

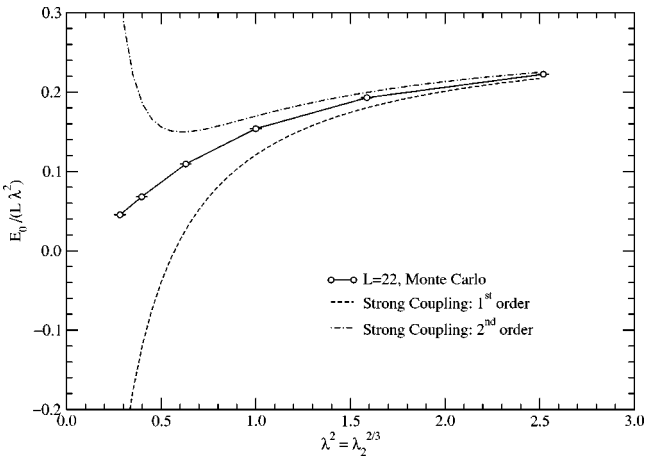

FIG. 3. Comparison between strong coupling and MC simulation for the ground state energy in the quadratic model with $V(\varphi)=\lambda_2\varphi^2$ on a lattice with $L=22$ spatial sites.

reached. For this reason, a full simulation of the model appears to be the only way to answer the question of symmetry breaking.

IV. RENORMALIZATION GROUP TRAJECTORIES

The action of the WZ model is

$$S=\int d^2x\left(\frac{1}{2}(\partial\varphi)^2+\frac{i}{2}\bar{\psi}\partial\psi-\frac{1}{2}V(\varphi)^2-\frac{1}{2}V'(\varphi)\bar{\psi}\psi\right).$$

At the perturbative level, this is a superrenormalizable field theory that can be made finite by a renormalization of $V(\varphi)$. In the minimal subtraction scheme the renormalized potential is obtained by solving the heat equation [25]

$$\mu\frac{\partial}{\partial\mu}V(\varphi,\mu)=-\frac{1}{4\pi}\frac{\partial^2}{\partial\varphi^2}V(\varphi,\mu), \tag{4.1}$$

where μ is the dimensional regularization scale. A dependence on μ is thus introduced in the coefficients of the various monomials appearing in the tree level $V(\varphi)$. For the specific case of $V(\varphi)=\lambda_2\varphi^2+\lambda_0$, we find that λ_2 is scale-independent and

$$\lambda_0(\mu)=\lambda_0(\mu_0)-\frac{\lambda_2}{2\pi}\log\frac{\mu}{\mu_0}.$$

On the lattice, let us denote by a hat the adimensional lattice coupling constants and by the label ''ph'' the physical ones, fixed and with dimension 1. The above result leads to

$$a\lambda_2^{\rm ph}=\hat{\lambda}_2 \tag{4.2}$$

$$a\lambda_0^{\rm ph}=\hat{\lambda}_0-\frac{\hat{\lambda}_2}{2\pi}\log aM. \tag{4.3}$$

The way we read these equations is as follows: at one loop and for small enough a, the physical λ_0 is obtained by compensating $\hat{\lambda}_0$ by the effect of the one-loop diagrams. These are computed with the UV cutoff a and with the IR cutoff given by the (dimension 1) mass M of the virtual particles in the loop.

The first equation allows to replace a by $\hat{\lambda}_2$ everywhere and we get

$$\hat{\lambda}_2=a\lambda_2^{\rm ph} \tag{4.4}$$

$$\hat{\lambda}_0=\hat{\lambda}_2\frac{\lambda_0^{\rm ph}}{\lambda_2^{\rm ph}}+\frac{\hat{\lambda}_2}{2\pi}\log\left(\hat{\lambda}_2\frac{M}{\lambda_2^{\rm ph}}\right). \tag{4.5}$$

This seems to show that the continuum limit can be reached with $\hat{\lambda}_2\to 0$ and

$$\frac{\hat{\lambda}_0}{\hat{\lambda}_2}\overset{\hat{\lambda}_2\to 0}{\sim} A+\frac{1}{2\pi}\log\hat{\lambda}_2 \tag{4.6}$$

where A contains the ratio $\lambda_2^{\rm ph}/\lambda_0^{\rm ph}$ and the details of the physical mass generation.

V. SIMULATION ALGORITHM

A. Green function Monte Carlo: General considerations

In this section, we review the Green function Monte Carlo approach to the study of the ground state of a general quantum model. To this aim, we consider the simple case of $(0+1)$-dimensional quantum mechanics in order to illustrate the basic ideas without unnecessary details hiding the essential features of the algorithm.

For a canonical spinless quantum particle, the Hamiltonian is

$$H=\frac{1}{2}p^2+V(q),\quad [q_i,p_j]=i\delta_{i,j}. \tag{5.1}$$

The ground state $|\Psi_0\rangle$ of H can be projected out of any initial state $|i\rangle$ with nonzero overlap $\langle\Psi_0|i\rangle\neq 0$. The projection is performed by applying the evolution semigroup $\{\exp(-tH)\}_{t\geqslant 0}$ and going to asymptotically large times.

Focusing on the ground state energy E_0, this procedure leads to the following simple formula:

$$E_0=\lim_{t\to+\infty}\frac{\langle f|He^{-tH}|i\rangle}{\langle f|e^{-tH}|i\rangle}; \tag{5.2}$$

the final state $|f\rangle$ is in principle arbitrary, as long as it is not orthogonal to $|\Psi_0\rangle$; in practice, it must be chosen with care, to avoid numerical instability.

The vacuum expectation value of a generic observable O can be computed as

$$\langle \Psi_0|O|\Psi_0\rangle = \lim_{t,\tau\to\infty} \frac{\langle f|e^{-\tau H}Oe^{-tH}|i\rangle}{\langle f|e^{-(\tau+t)H}|i\rangle}; \tag{5.3}$$

this procedure is known as *forward walking*.

To translate the above formula into a stable numerical algorithm, it is necessary to find a basis such that the Hamiltonian H has nonpositive off-diagonal matrix elements. By the way, this is true for the Hamiltonian (5.1) in the basis $\{|q\rangle\}$ of position eigenstates. If such a basis is found, it is possible to identify matrix elements of e^{-tH} as probability transitions defining a Markov random process in the state space. For instance, in the simple case when $|f\rangle$ is chosen to be a zero momentum state, $p|f\rangle = 0$, we have (Feynman-Kac formula)

$$\begin{aligned} E_0 &= \lim_{t\to+\infty} \frac{\langle f|Ve^{-tH}|i\rangle}{\langle f|e^{-tH}|i\rangle} \\ &= \lim_{t\to+\infty} \frac{\int \mathcal{D}q(\tau)V[q(t)]e^{-\int_0^t V[q(\tau)]d\tau}}{\int \mathcal{D}q(\tau)e^{-\int_0^t V[q(\tau)]d\tau}}, \end{aligned} \tag{5.4}$$

where $\mathcal{D}q(\tau)$ is the Wiener measure.

The probabilistic interpretation of the above equation is as follows: E_0 (as well as other observables) can be computed by taking the average over weighted walkers which diffuse according to the Wiener process. Each path is weighted by the following functional of the trajectory:

$$W[q(\tau)] = \exp - \int_0^t V[q(\tau)]d\tau. \tag{5.5}$$

In the numerical implementation, an estimate of E_0 is obtained by computing

$$\lim_{t\to+\infty} \frac{\mathbf{E}[V(\hat{q}_t)\hat{W}_t]}{\mathbf{E}(\hat{W}_t)}, \tag{5.6}$$

where $\hat{q}_t$ is a numerical discretization of the Wiener process, $\hat{W}_t$ its associated weight computed by properly approximating Eq. (5.5) and, finally, $\mathbf{E}(\cdot)$ denotes the average with respect to the realizations of $\hat{q}_t$. In practice, after the choice of a particular approximation $\hat{q}_t$, one works with a large number K of walkers and extrapolates numerically to $K \to \infty$. The control of the approximations involved in this strategy requires some discussion that we defer to the section devoted to results.

A point that is worth mentioning regards the possibility of introducing a guidance in the walkers diffusion. To improve the convergence to ground state it is customary to define the unitarily equivalent Hamiltonian

$$\tilde{H} = e^S H e^{-S} = \frac{1}{2}p^2 + ip\cdot F + \tilde{V}(q), \tag{5.7}$$

where S is an arbitrary (real) function and

$$\begin{aligned} F &= \nabla S, \\ \tilde{V} &= V - \frac{1}{2}(\nabla S)^2 - \frac{1}{2}\Delta S. \end{aligned} \tag{5.8}$$

It can be shown that the derivation of expressions like Eq. (5.4) can be easily generalized to this case and the required modifications can be summarized as (i) the potential V is replaced by $\tilde{V}$, (ii) the Wiener process is replaced by a deformed process guided by the drift F. In the following, we shall call importance sampling the trick of exploiting a nonzero S.

In the following sections, we describe in full details the algorithm for the model under study considering first the bosonic and fermionic sectors separately and finally the full Hamiltonian.

B. Bosonic sector

The bosonic sector of the lattice model is a canonical quantum mechanical one with many degrees of freedom. The algorithm is the one described in the previous section. Given the transformed Hamiltonian $\tilde{H}$ of Eq. (5.7), we write

$$\begin{aligned} \exp(-\varepsilon\tilde{H}_B) = \exp\left(-\frac{\varepsilon}{2}\tilde{V}\right)\exp\left(-\frac{\varepsilon}{2}\frac{p^2}{2}\right)e^{-i\varepsilon p\cdot F} \\ \times \exp\left(-\frac{\varepsilon}{2}\frac{p^2}{2}\right)\exp\left(-\frac{\varepsilon}{2}\tilde{V}\right) + \mathcal{O}(\varepsilon^3). \end{aligned} \tag{5.9}$$

The function $\tilde{V}$ depends on the bosonic state, i.e. the set of values of the scalar fields that we collectively denote by Q.

The rule for the update of the weighted walker (Q,W) is built, step by step, following the approximate operator factorization (5.9) and reads (see [26] for similar calculations in the solution of the Langevin equation)

$$(Q',W') \to (Q''',W'''), \tag{5.10}$$

where Q''' and W''' are built according to

$$W'' = W'\exp\left(-\frac{\varepsilon}{2}\tilde{V}(Q')\right), \tag{5.11}$$

$$Q'' = Q' + \sqrt{\frac{\varepsilon}{2}}\xi',$$

$$z = Q' + \frac{\varepsilon}{2}F(Q'),$$

$$Q'' = Q' + \varepsilon F(z),$$

$$Q''' = Q'' + \sqrt{\frac{\varepsilon}{2}}\xi'',$$

$$W''' = W''\exp\left(-\frac{\varepsilon}{2}\tilde{V}(Q''')\right),$$

and ξ', ξ'' are independent sets of Gaussian random numbers. In the above update, the integration of the equations of motion associated with the driving force F has been solved at second order. In the end a systematic error $\mathcal{O}(\varepsilon^3)$ with respect to the evolution time has been introduced.

An estimate of the energy in the bosonic sector is obtained by taking the weighted average of $\tilde{V}$ over several realizations of the walker path

$$E_0^{\text{bosonic}} = \lim_{t\to+\infty}\frac{\mathbf{E}[\tilde{V}(Q_t)W_t]}{\mathbf{E}(W_t)}. \tag{5.12}$$

C. Fermionic sector

In the fermionic sector, the spirit of the algorithm is the same, but there are important technical differences that we want to emphasize. At fixed scalar fields configuration, the remaining state space is purely fermionic and, on a finite lattice, it is both discrete and finite dimensional.

To simplify notation, in this section we denote $H \equiv H_F$. The Hamiltonian can be thought of as a large sparse matrix $H = \|H_{ss'}\|$ with s and s' denoting fermionic states. We now show that a similar construction like the one exploited with H_B can be repeated here. The Gaussian random noise that was the building block in the simulation of the Wiener process is replaced here by a discrete jump process.

Again, the problem is that of giving a probabilistic representation for the evolution semigroup $\Omega = \{e^{-tH}\}_{t\geq 0}$. To this aim, we define a Markov process that describes diffusion in the discrete state space and we also provide a rule for the update of a walker weight. We finally show that suitable averages over weighted walkers reconstruct the evolution governed by H and project a given initial state onto the ground state.

For each pair s, s' in the state space S such that $s \neq s'$ and $H_{s's} \neq 0$ we define $\Gamma_{s's} = -H_{s's}$. We assume that all $\Gamma_{s's} > 0$ (no sign problem) and build an S-valued Markov stochastic process s_t by identifying $\Gamma_{s's}$ as the rate for the transition $s \to s'$. Hence, the average occupation $P_s(t) = \mathbf{E}(\delta_{s,s_t})$, with $\mathbf{E}(\cdot)$ denoting the average with respect to s_t, obeys the Master Equation $\dot{P}_s(\beta) = \Sigma_{s'\neq s}(\Gamma_{ss'}P_{s'} - \Gamma_{s's}P_s)$.

Related to s_t, we also define the real valued stochastic process $W_t = \exp(-\int_0^t \omega_{s_t} dt)$, with $\omega_s = \Sigma_{s'\in S} H_{s's}$. It can be shown that the weighted expectation value $\psi_s(t) = \mathbf{E}(\delta_{s,s_t}W_t)$ reconstructs Ω,

$$\frac{d}{dt}\psi_s(t) = -\sum_{s'\in S} H_{ss'}\psi_{s'}(t),$$

with $\psi_s(0) = \text{Prob}(s_0 = s)$. Matrix elements of Ω can be identified with certain expectation values. In particular, the ground state energy E_0 (in the purely fermionic sector) can be obtained by

$$E_0 = \lim_{t\to+\infty}\frac{\mathbf{E}(\omega_{s_t}W_t)}{\mathbf{E}(W_t)}. \tag{5.13}$$

The actual construction of the process is straightforward. A realization of s_t is a piece-wise constant map $\mathbf{R} \to S$ with isolated jumps at times $t = t_0, t_1, \ldots,$ with $t_0 < t_1 < t_2 < \cdots$. The algorithm that computes the triples $\{t_n, s_{t_n}, W_{t_n}\}$ is the following:

(i) We denote $s_{t_n} \equiv s$ and define the set T_s of target states connected to s: $T_s = \{s', \Gamma_{s's} > 0\}$. We also define the total width $\Gamma_s = \Sigma_{s'\in T_s}\Gamma_{s's}$.

(ii) Extract $\tau \geq 0$ with probability density $p_s(\tau) = \Gamma_s e^{-\Gamma_s \tau}$. In other words, $\tau = -(1/\Gamma_s)\log\xi$ with ξ uniformly distributed in $[0,1]$.

(iii) Extract a new state $s' \in T_s$ with probability $p_{s'} = \Gamma_{s's}/\Gamma_s$.

(iv) Define $t_{n+1} = t_n + \tau$, $s_{t_{n+1}} = s'$ and $W_{t_{n+1}} = W_{t_n}\cdot e^{-\omega_s \tau}$.

In this sector there is no systematic error due to a finite evolution time. The semigroup dynamics is in fact reproduced exactly by the above stochastic process (s_t, W_t).

About Importance Sampling, we remark that in the discrete case, the inclusion of a trial wave function amounts to the redefinition

$$\tilde{H}_{s's} = \Psi_{s'}^T H_{s's}\frac{1}{\Psi_s^T}, \tag{5.14}$$

where $\Psi_s^T = \langle s|\Psi_0^T\rangle$ are the components of the trial ground state $|\Psi_0^T\rangle$. The new Hamiltonian $\tilde{H}$ is not symmetric, but the above formulas works as well with no need for further modifications: actually, they have been derived without requiring any symmetry condition $H = H^T$.

Some final comments are in order about the choice of the basis for the fermionic states. As we mentioned in the general discussion, we want to have zero or negative off-diagonal matrix elements of H. The simplest choice amounts to consider eigenstates $|\boldsymbol{n}\rangle$ of the occupation numbers $\chi_i^\dagger\chi_i$ and with a relative phase fixed by the natural choice

$$|\boldsymbol{n}\rangle = \prod_{i=1}^{L}(\chi^\dagger)^{n_i}|0\rangle, \quad \chi_i|0\rangle = 0. \tag{5.15}$$

This does not guarantee that the above sign problems are absent. In fact, in weak-coupling perturbation theory, the choice of periodic boundary conditions does not break supersymmetry when $L \bmod 4 = 0$ as can be checked, e.g., in the free model. However, under this condition, there is an even number of fermions, $L/2$, in the ground state and a sign problem arises due to boundary crossings of a fermion, since such a transition involves an odd number of fermion exchanges. To avoid such a difficulty, we shall adopt open boundary conditions. With this choice, L needs just to be even to assure a supersymmetric weak coupling ground state. Also, we shall restrict to the case $L \bmod 4 = 2$ and to the sector with $L/2$ fermions that contains a nondegenerate ground state, with zero energy at all orders in a weak-coupling expansion.

D. Algorithm for the full model

To study the full Hamiltonian of the Wess-Zumino model, the simplest attitude is to perform an approximate splitting of the bosonic and fermionic sectors. For instance, with second order precision, we can write

$$\exp(-\varepsilon H) = \exp\left(-\frac{1}{2}\varepsilon H_B\right)\exp(-\varepsilon H_F) \times \exp\left(-\frac{1}{2}\varepsilon H_B\right) + \mathcal{O}(\varepsilon^3), \qquad (5.16)$$

and consider separately the evolution related to H_B and H_F freezing the fermionic or bosonic fields respectively. In the end, an extrapolation to the $\varepsilon \to 0$ limit must be performed. Equation (5.16) has been approximated to the same order as Eq. (5.9); if necessary, both can be improved.

E. Variance control

A straightforward implementation of the above formulas fails because of a numerical instability: the variance of the walker weights W_t computed over the walkers ensemble grows exponentially with t and forbids the projection onto the ground state [27]. A good trial wave function can certainly reduce the growth rate, but the problem disappears only in the ideal case when the trial wave function is exact. To bypass this problem, some kind of *branching* procedure must be applied in order to delete trajectories (walkers) with low weight and replicate those with larger weight.

In practice, we introduce an ensemble, i.e., a collection of K independent walkers $s^{(n)}$ each one carrying its own weight $W^{(n)}$:

$$\mathcal{E} = \{(s^{(n)}(t), W^{(n)}(t)), 1 \leqslant n \leqslant K\}. \qquad (5.17)$$

When the variance of the weights in the ensemble becomes too large, $\mathcal{E}$ is transformed in a new ensemble $\mathcal{E}'$ that reproduces the same expectation values (at least in the $K \to \infty$ limit) and has a smaller variance. We adopted the branching procedure of Ref. [28]: for each walker $s^{(n)}$ we compute a multiplicity

$$M^{(n)} = \lfloor c W^{(n)} + \xi \rfloor, \quad c = \frac{\overline{K}}{\sum_n W^{(n)}}, \qquad (5.18)$$

where ξ is a random number uniformly distributed in $[0,1]$, $\overline{K}$ is the desired number of walkers, and $\lfloor x \rfloor$ is the maximum integer not greater than x; the new ensemble $\mathcal{E}'$ contains $M^{(n)}$ copies of each configuration $s^{(n)}$ in $\mathcal{E}$ and all the weights are set to 1; the actual number of walkers K will oscillate around $\overline{K}$. This procedure has the advantage that there is no harmful effect from its repeated application; therefore we apply it at each Monte Carlo iteration, after all the fields have been updated.

F. Choice and dynamical optimization of the trial wave function Ψ_T

About the choice of the trial wave function, we propose the factorized form

$$|\Psi_0^T\rangle = e^{S_B(\varphi) + S_F(\varphi, \chi, \chi^\dagger)} |\Psi_0\rangle_B \otimes |\Psi_0\rangle_F, \qquad (5.19)$$

where $|\Psi_0\rangle_B \otimes |\Psi_0\rangle_F$ is the ground state of the free model given explicitly in Appendix D and

$$S_B = \sum_n \sum_{k=1}^{d_B} \alpha_k^B \varphi_n^k,$$

$$S_F = \sum_n (-1)^n \left(\chi_n^\dagger \chi_n - \frac{1}{2}\right) \sum_{k=1}^{d_F} \alpha_k^F \varphi_n^k.$$

Since the trial wave function is a modification of the free ground-state wave function, we expect that importance sampling will improve as we approach the continuum limit.

The degrees d_B and d_F must be chosen carefully to achieve a balance between the accuracy of the trial wave function on one hand, and convergence of the adaptive determination of the parameters α and computation time on the other hand. We chose $d_B = d_F = 4$, except for situations very close to the continuum limit, e.g., $V = \lambda_2 \varphi^2 + \lambda_0$ with $\lambda_2 < 0.2$, for which we chose $d_B = d_F = 2$ (cf. Sec. VI D).

The trial wave function should of course respect the symmetries of the model; a Z_2 symmetry possessed by the model for specific forms of V is very helpful to reduce the number of parameters that we must optimize. For odd V, the model enjoys the exact symmetry $\varphi_n \to -\varphi_n$, and therefore odd α_k^B and α_k^F can be set to zero. For even V, the model enjoys the approximate symmetry $\varphi_n \to -\varphi_n$, $\chi_n \leftrightarrow \chi_n^\dagger$ (it is broken by irrelevant terms and by boundary terms), and we verified that odd α_k^B and even α_k^F can be set to zero.

Let us denote by $\boldsymbol{\alpha} = \{\alpha^B, \alpha^F\}$ the collective set of free parameters appearing in the trial wave function. A possible approach consists in performing simulations of moderate size at fixed $\boldsymbol{\alpha}$ in order to optimize their choice. However, as shown in [29], the trial wave function $|\Psi_0^T\rangle$ can also be optimized dynamically within Monte Carlo evolution with a better performance of the full procedure.

The idea is again simple: consider the ground state energy as a typical observable; for a given choice of $\boldsymbol{\alpha}$, after N Monte Carlo steps, a simulation with an average population of K walkers furnishes a biased estimator $\hat{E}_0(N,K,\boldsymbol{\alpha})$. If we denote by $\langle\cdot\rangle$ the average with respect to Monte Carlo realizations, $\hat{E}_0$ is a random variable such that

$$\lim_{N\to\infty}\langle\hat{E}_0(N,K,\boldsymbol{\alpha})\rangle = E_0 + \delta E_0(\boldsymbol{\alpha},K), \tag{5.20}$$

where $\delta E_0(\boldsymbol{\alpha},K)$ depends on $\boldsymbol{\alpha}$, but vanishes as $K\to\infty$. Besides, the size of the fluctuations is measured by

$$\mathrm{Var}\,\hat{E}_0(N,K,\boldsymbol{\alpha}) \overset{N\to\infty}{\sim} \frac{c_2(K,\boldsymbol{\alpha})}{\sqrt{N}}. \tag{5.21}$$

In the $K\to\infty$ limit, $\langle\hat{E}_0\rangle$ is exact and independent of $\boldsymbol{\alpha}$. The constant $c_2(K,\boldsymbol{\alpha})$ is related to the fluctuations of the effective potential $\tilde{V}$ and is strongly dependent on $\boldsymbol{\alpha}$. The problem of finding the optimal trial wave function can be translated in the minimization of $c_2(K,\boldsymbol{\alpha})$ with respect to $\boldsymbol{\alpha}$.

The algorithm we propose performs this task by interlacing a Stochastic Gradient steepest descent with the Monte Carlo evolution of the walkers ensemble. At each Monte Carlo step, we update $\boldsymbol{\alpha}_n \to \boldsymbol{\alpha}_{n+1}$ according to the simple law

$$\boldsymbol{\alpha}_{n+1} = \boldsymbol{\alpha}_n - \eta_n \nabla_{\boldsymbol{\alpha}} \mathrm{Var}_{\mathcal{E}_n}\tilde{V} \tag{5.22}$$

where $\mathcal{E}_n$ is the ensemble at step n and $\{\eta\}$ is a suitable sequence, asymptotically vanishing; to keep things simple, we use the same η for all components α_k of $\boldsymbol{\alpha}$, although in principle we could use a different η_k for each α_k.

A nonlinear feedback is thus established between the trial wave function and the evolution of the walkers. The convergence of the method cannot be easily investigated by analytical methods and explicit numerical simulations are required to understand the stability of the algorithm. In [29], examples of applications of the method with purely bosonic or fermionic degrees of freedom can be found. Here, we apply the method for the first time to a model with both kinds of fields.

In practice, the choice of the initial values of $\boldsymbol{\alpha}$ is important: it is clear that, if we have a good guess of the optimal values (e.g., from runs at the same V but for smaller values of L or K), starting from them makes the convergence much faster. We also noticed that, starting e.g. from $\boldsymbol{\alpha}_0 = 0$, the steepest descent at times fails and $\boldsymbol{\alpha}_n$ oscillates wildly; this never happens if most of the starting values have at least the right sign and order of magnitude.

We found it useful to determine η dynamically as well. The basic idea is that we wish to decrease η when all the α_k have reached the optimal value and they are oscillating at random around it: in this situation, a smaller η means less noise on $\boldsymbol{\alpha}$. On the other hand, we wish to increase η when one or more α_k is drifting: a larger η now means a faster approach toward the optimal value. To monitor the trend of $\boldsymbol{\alpha}$, we use the quantity

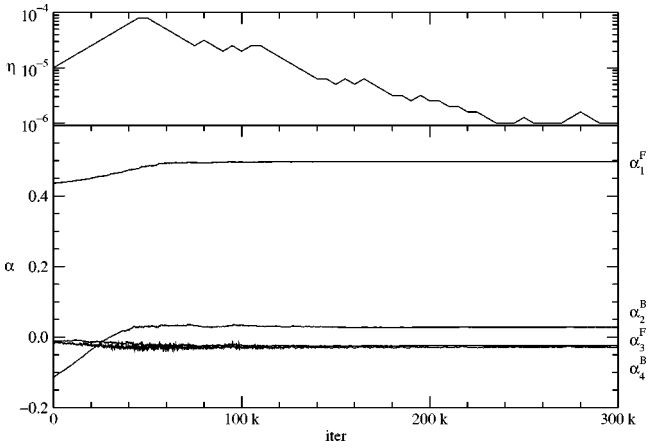

FIG. 4. $\boldsymbol{\alpha}$ and η dynamics from a run at $V = 0.5\varphi^2 - 0.55$, $L = 34$ and $K = 100$.

$$\tau = \max_k \tau_k, \quad \tau_k = \frac{N|a_k|}{v_k} - 3, \tag{5.23}$$

where $N = n_1 - n_0$ is the number of iterations in the interval of Monte Carlo iterations $(n_0,n_1]$ we are considering, v_k is the variance of α_k in the interval, and a_k is the slope of the linear least-squares fit to $\alpha_{k,n}$ vs n. τ_k is invariant under translations and scale transformations; it is positive if α_k is drifting and it is negative if α_k is oscillating.

A typical example of the implementation of the $\boldsymbol{\alpha}$ and η dynamics is shown in Fig. 4; η is initialized to 10^{-5}; after each interval of $N = 5000$ iterations, if $\tau > 0.15$, η is multiplied by $\sqrt[10]{10}$; if $\tau < 0$, η is divided by $\sqrt[10]{10}$; if $0 < \tau < 0.15$, η is unchanged; finally, η is restricted to the interval $[10^{-6},10^{-4}]$. The parameters of the η dynamics given here were obtained empirically.

G. Observable measurement

We measure the vacuum expectation values of φ_n, $\varphi_n\varphi_m$, $\chi_n^\dagger\chi_n$, and of

$$T = \frac{1}{2}\sum_{n=1}^{L}(\varphi_{n+1} - \varphi_{n-1})V(\varphi_n),$$

$$Y_q = \left\{ Q, \sum_{n=1}^{L} \varphi_n^q \psi_{2,n} \right\}. \tag{5.24}$$

Note that, with our choice of boundary conditions, we do not have translation invariance and, e.g., $\langle\varphi_n\rangle$ will depend on i; however, the dependence is sizable only within a few correlation lengths from the border; therefore we typically average site-dependent quantities excluding sites closer than a suitable $L_{\min}$ from the border; in the case of $\langle\varphi_n\varphi_m\rangle$, we average over all pairs with fixed distance $r = |n-m|$, excluding the cases when n or m is closer than $L_{\min}$ from the border.

The ground-state energy is measured simply by averaging the measured values of E_0 over the ensembles $\mathcal{E}(t)$, discarding a suitable thermalization interval $(0,t_0)$:

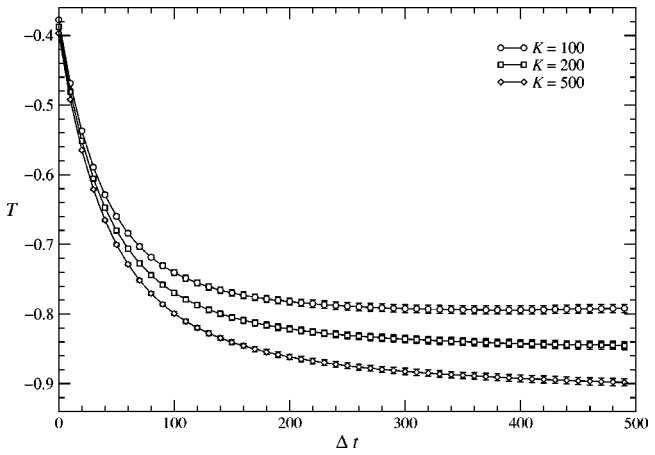

FIG. 5. The central charge T [cf. Eq. (5.24)] vs Δt from runs at $V=0.5\varphi^2$ and $L=34$.

$$E_0 \cong \frac{1}{t_1-t_0}\sum_{t=t_0+1}^{t_1}\frac{\sum_{i=1}^{K_t} E_{i,t}w_{i,t}}{\sum_{i=1}^{K_t} w_{i,t}},$$

$$E_{i,t}=\frac{\langle s_{i,t}|H|s_{i,t}\rangle}{\langle s_{i,t}|s_{i,t}\rangle}, \tag{5.25}$$

cf. Eq. (5.2). The vacuum expectation value of a generic observable is computed implementing the forward-walking formula (5.3) as

$$\langle O\rangle \cong \frac{1}{t_1-t_0}\sum_{t=t_0+1}^{t_1}\frac{\sum_{i=1}^{K_t} O_{i,t}w_{i,t+\Delta t}}{\sum_{i=1}^{K_t} w_{i,t+\Delta t}},$$

$$O_{i,t}=\frac{\langle s_{i,t}|O|s_{i,t}\rangle}{\langle s_{i,t}|s_{i,t}\rangle}. \tag{5.26}$$

In principle, in Eq. (5.26) we must take the $\Delta t\to\infty$ limit, but in practice a moderate value like $\Delta t=500$ is sufficient. A typical example of Δt dependence is shown in Fig. 5; it should be noticed that the error bars grow with Δt but very slowly.

VI. NUMERICAL RESULTS

A. Review of previous lattice studies

The class of models that we study in this paper has been previously considered in [18] with a Monte Carlo approach that determines the ground state energy by using

$$E_0=\lim_{\beta\to\infty}\frac{\mathrm{Tr}(He^{-\beta H})}{\mathrm{Tr}(e^{-\beta H})}, \tag{6.1}$$

and working numerically with a large fixed β. This is in the spirit of the usual Lagrangian algorithms to be compared with the Green function Monte Carlo method where β can be identified with the simulation time and is thus taken to infinity by the very nature of the algorithm.

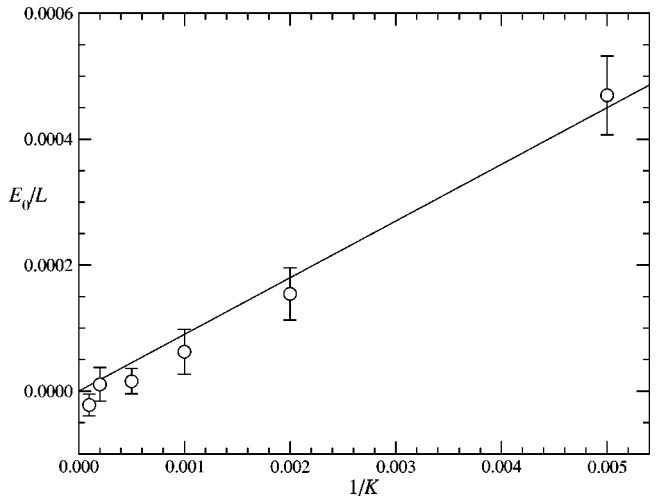

FIG. 6. The ground-state energy density E_0/L vs $1/K$ at $V=\varphi^3$, $L=22$, with statistics of 1 M iterations for $K<5000$, 500 k iterations at $K=5000$, and 300 k iterations at $K=10000$.

The analysis of [18] is performed on a 12×100 lattice, hence with a rather coarse spatial mesh. In the model with $V(\varphi)=\lambda_3\varphi^3$, supersymmetry appears to be unbroken in full agreement with our analysis. In the quadratic model with $V(\varphi)=\lambda_2\varphi^2+\lambda_0$, the authors of Ref. [18] find rather strong signals for supersymmetry breaking with λ_0 bigger that the critical value $\lambda_0\simeq-0.5$ and have numerical results showing a very small ground state energy for $\lambda_0<-0.5$. No discussion of the continuum limit is attempted.

B. Odd V

As an example of odd prepotential, we study the case $V=\varphi^3$. We plot the ground-state energy vs K in Fig. 6 and the Ward identity Y_1 vs K in Fig. 7. Both give very convincing evidence for unbroken SUSY; all the other Ward identities

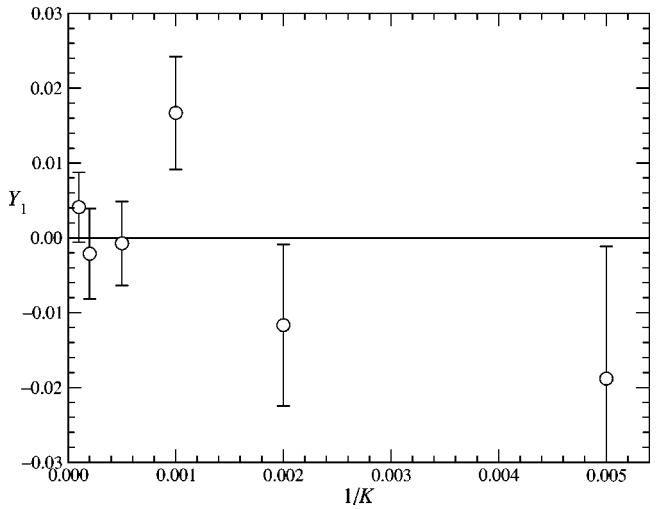

FIG. 7. The Ward identity Y_1 vs $1/K$ at $V=\varphi^3$, $L=22$.

are consistent with zero, but more noisy. It should be noticed that the bosonic and fermionic contribution to E_0 are $\simeq \pm 7.4$: we are observing a cancellation of four orders of magnitude.

C. Supersymmetry breaking

We now turn to the more interesting case of even prepotential, investigating the case $V=\lambda_2\varphi^2+\lambda_0$. We remind that in this case the model enjoys an approximate Z_2 symmetry $\varphi_n \to -\varphi_n$, $\chi_n \leftrightarrow \chi_n^\dagger$. For fixed λ_2, we may expect (in the $L\to\infty$ limit) a phase transition at $\lambda_0=\lambda_0^{(c)}(\lambda_2)$, separating a phase of broken SUSY and unbroken Z_2 (high λ_0) from a phase of unbroken SUSY and broken Z_2 (low λ_0). We investigated in details the case $\lambda_2=0.5$.

The usual technique for the study of a phase transition is the *crossing* method, applied to the Binder cumulant [30]

$$B=\frac{1}{2}\left(3-\frac{\langle M^4\rangle}{\langle M^2\rangle^2}\right); \tag{6.2}$$

in our case, the choice of a sensible definition for the magnetization M is nontrivial, since our model is neither ferromagnetic nor antiferromagnetic, and it does not enjoy translation symmetry. We tried out several definitions, before making the choice

$$M_{\text{even (odd)}} \equiv \frac{2}{L-2L_{\min}} \sum_{\text{even(odd)}i=1+L_{\min}}^{L-L_{\min}} \phi_i, \tag{6.3}$$

where, typically, $L_{\min}=6$; M_{even} and M_{odd} are perfectly equivalent, and the values of B we quote in the following are the average of B_{even} and B_{odd}.

The crossing method consists in plotting B vs λ_0 for several values of L; the crossing point $\lambda_0^{\text{cr}}(L_1,L_2)$, determined by the condition

$$B(\lambda_0^{\text{cr}},L_1)=B(\lambda_0^{\text{cr}},L_2),$$

is an estimator of $\lambda_0^{(c)}$ [30]; the convergence is dominated by the critical exponent ν of the correlation length and by the critical exponent ω of the leading corrections to scaling (cf. Ref. [31]):

$$\lambda_0^{\text{cr}}(L_1,L_2)=\lambda_0^{(c)}+O(L_1^{-\omega-1/\nu},L_2^{-\omega-1/\nu});$$

we expect the phase transition we are studying to be in the Ising universality class, for which $\nu=1$ and $\omega=2$, and therefore we expect fast convergence of λ_0^{cr} to $\lambda_0^{(c)}$. The results, plotted in Fig. 8, indicate $\lambda_0^{(c)}=-0.48\pm 0.01$.

It is possible to study the phase transition by looking at the connected correlation function $G_d=\langle \varphi_n\varphi_m\rangle_c$, averaged over all n,m pairs with $|m-n|=d$, excluding pairs for which m or n is closer to the border than (typically) 6. In our staggered formulation, even and odd d may correspond to different physical channels.

G_d is fitted to the form $\exp[-a_1-a_2 d+a_3/(d+10)]$, separately for even and odd d; the best fits give a good χ^2 if we remove the smallest distances, typically $d\leqslant 3$ for the odd channel and $d\leqslant 4$ for the even channel. In the broken phase,

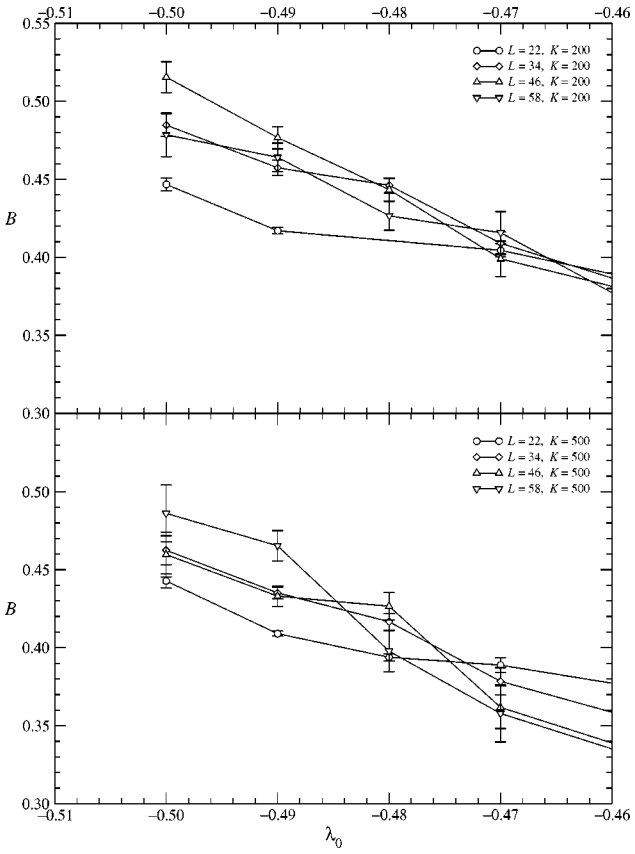

FIG. 8. The Binder cumulant B vs λ_0.

we have small but nonzero a_2, and we observe equivalence of the even- and odd-d channels; an example is shown in Fig. 9. In the unbroken phase, a_2 is larger, and the even- and odd-d channels are somewhat different; an example is shown in Fig. 10. The difference between the two phases is apparent, e.g., in the plot of a_2 vs λ_0, presented in Fig. 11; the data presented here would indicate $\lambda_0^{(c)}=-0.48\pm 0.01$.

An alternative window to the phase transition is offered by the optimized values of the parameters of the bosonic part of the trial wave function, which should be related to the

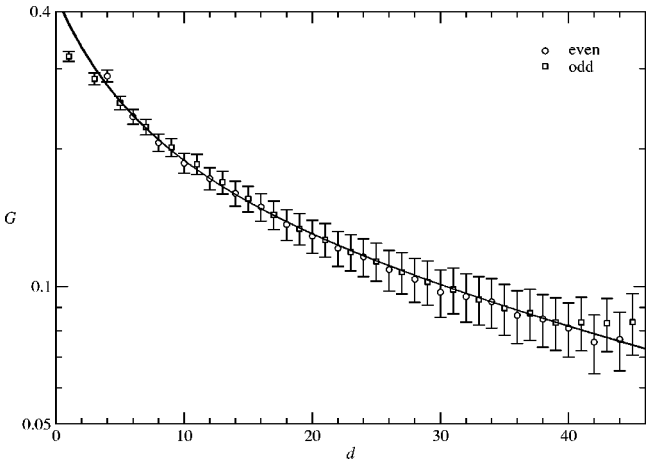

FIG. 9. The connected correlation function G_d for $V=0.5\varphi^2-0.5$.

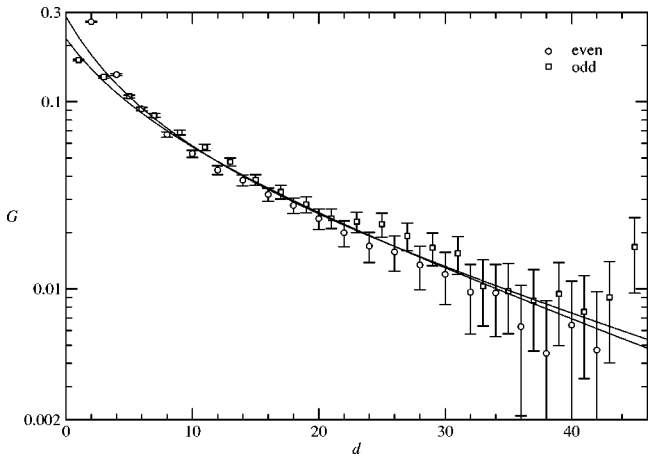

FIG. 10. The connected correlation function G_d for $V=0.5\varphi^2-0.38$.

effective potential $V_{\rm eff}$ of the bosonic field,

$$V_{\rm eff}(\varphi)\sim-\alpha_4^B\varphi^4-\alpha_2^B\varphi^2;$$

we verified that $\alpha_4^B<0$, as required by stability; a negative value for α_2^B therefore indicates unbroken Z_2 symmetry, while a positive α_2^B indicates spontaneous breaking of Z_2.

The numerical values of α_2^B are shown in Fig. 12. It is clear that, especially in the broken phase, statistical errors are underestimated. The above-mentioned scenario is qualitatively confirmed, but the data yield $\lambda_0^{(c)}\simeq-0.40$, which is very far from the more traditional estimates obtained above.

Finally, to investigate the supersymmetry properties of each phase, we analyze $\mathcal{E}$, the ground-state energy density extrapolated to infinite K and L. We fit E_0/L to the form

$$\frac{E_0}{L}=\mathcal{E}+\frac{a+bL}{K^\nu};\tag{6.4}$$

χ^2/d.o.f. (degrees of freedom) from 1 to 2; the errors on the fit parameters are defined by the values giving an increase of χ^2 by 1; if $\chi^2>$d.o.f. we multiply them by the "scale factor" $S=\sqrt{\chi^2/\text{d.o.f.}}$. We present a plot of $\mathcal{E}$ vs λ_0 in Fig. 13; these data give $\lambda_0^{(c)}\sim-0.53$, with a rather large uncertainty.

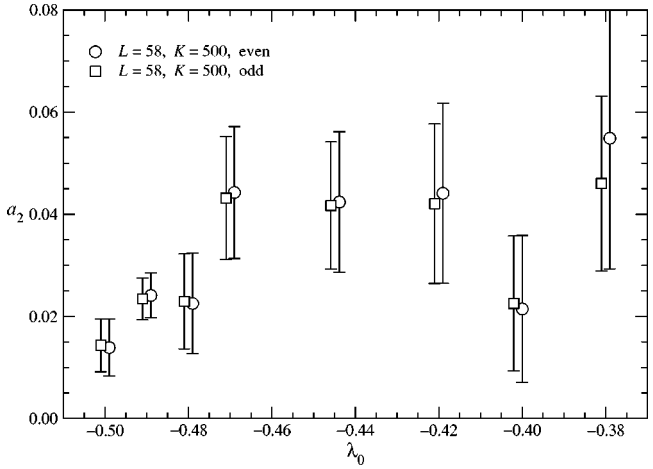

FIG. 11. The effective mass a_2 of G_d vs λ_0 for $L=58$ and $K=500$; for $\lambda_0\leqslant-0.51$ the error on a_2 is very large.

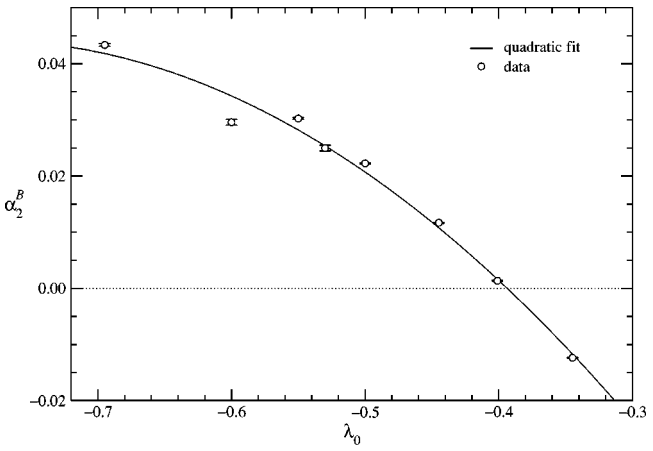

FIG. 12. The optimization parameter α_2^B; it is insensitive to L and K.

D. Continuum limit

We wish to investigate if the pattern established in Sec. VI C extends to the continuum limit.

We study the trajectory

$$\lambda_0=\frac{\lambda_2}{2\pi}\ln(4\lambda_2),\tag{6.5}$$

corresponding to a 1-loop RG trajectory, cf. Eq. (4.6); the effect of λ_0 is small in the range we considered, therefore we expect this to be a reasonable approximation to a true RG trajectory.

We estimate the correlation length from the exponential decay of the connected correlation function $G_d=\langle\varphi_n\varphi_m\rangle_c$ averaged over all n,m pairs with $|m-n|=d$, excluding pairs for which m or n is closer to the border than (typically) 8. In our staggered formulation, even and odd d correspond to different physical channels.

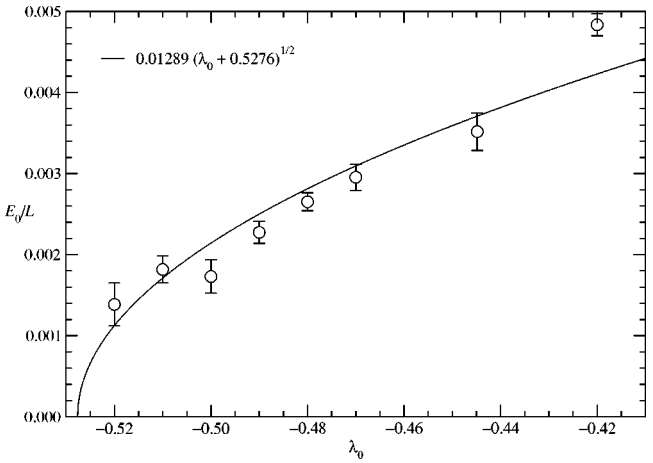

FIG. 13. The ground-state energy density E_0/L vs λ_0. The solid line is a fit to the form $E_0/L=a\sqrt{\lambda_0-\lambda_0^{(c)}}$.

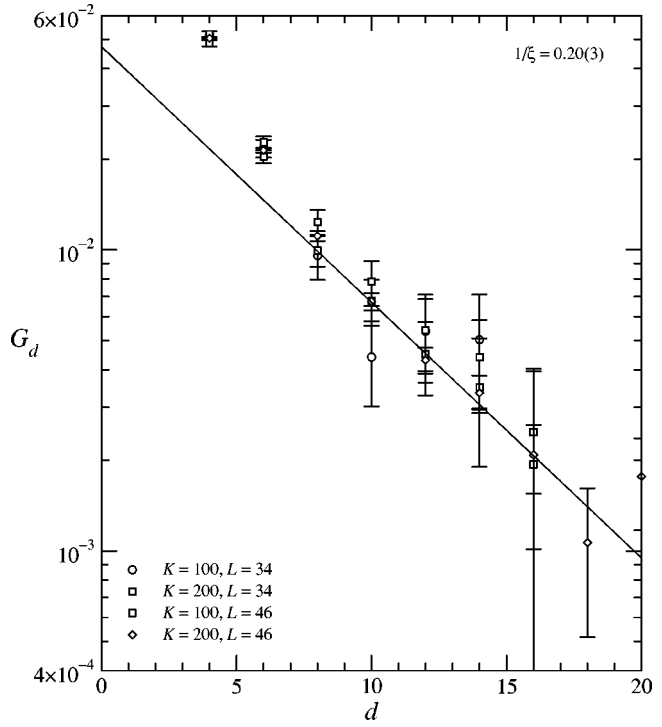

FIG. 14. The connected correlation function G_d at even distance for $V=0.353553\varphi^2+0.019502$; the curve and value of $1/\xi$ quoted are the result of an exponential fit for $10\leqslant d\leqslant 18$ to the $L=46$, $K=200$ data.

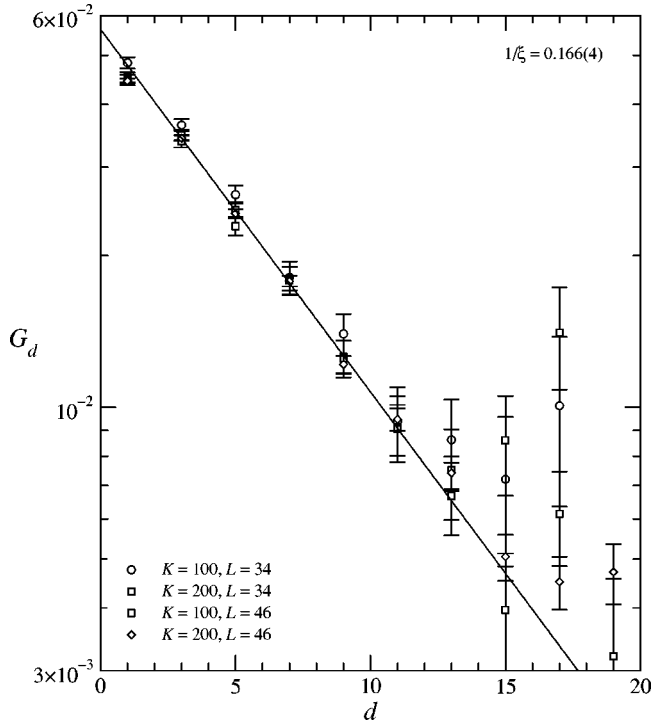

FIG. 15. The connected correlation function G_d at odd distance for $V=0.353553\varphi^2+0.019502$; the curve and value of $1/\xi$ quoted are the result of an exponential fit for $3\leqslant d\leqslant 15$ to the $L=46$, $K=200$ data.

We performed runs for values of λ_2 spaced by a factor of $\sqrt{2}$, with a statistics of 4×10^6 iterations. In Figs. 14 and 15 we show the plots of the φ correlation for the case $V=0.35\varphi^2+0.02$. It is very difficult to extract a correlation length from the even-d channel, presumably because φ has a very small overlap with the lightest state of the channel, and the value $1/\xi=0.20\pm0.03$ quoted in Fig. 14 should be considered tentative. The odd-d channel is much cleaner, and it is possible to estimate ξ with a good precision.

For the other values of λ_2, the situation is similar but with slightly larger errors. The measured values of $\xi_{\rm odd}$ follow very well the naïve scaling behavior

$$\xi\propto 1/\lambda_2 .$$

The entire range $0.088\leqslant\lambda_2\leqslant0.35$ seems to be in the scaling region, with $\lambda_2=0.5$ a borderline case, as shown in Fig. 16. The values of $\xi_{\rm even}$ have very large errors, and it is hard to draw any conclusion from them.

The Green function Monte Carlo algorithm gives a very accurate measurement of the ground-state energy E_0; to give a feeling of the precision reached, we quote the results for the smallest and the largest value of λ_2 we considered, along the trajectory (6.5),

$$E_0(\lambda_2=0.044,L=46,K=200)=(1.28\pm0.01)\times10^{-3};$$

$$E_0(\lambda_2=0.5,L=46,K=200)=(69.44\pm0.05)\times10^{-3}.$$

E_0 show a sizable dependence on K and L, and it is therefore necessary to perform an extrapolation to $L\to\infty$ and $K\to\infty$; we fitted the energy density to the form

$$\frac{E_0}{L}=\mathcal{E}+\frac{c}{L}+\frac{d}{L^2}+K^{\nu}\left(e+\frac{f}{L}\right),$$

which gives a good χ^2. ν remains constant within errors, with a value $\nu\approx0.75$, i.e., the algorithm performs well as we approach the continuum limit.

The ''scaling'' plot of the energy density E_0/L is shown in Fig. 17. It seems to behave as $\lambda_2^{1.7}$, while naïve scaling would predict $E_0/L\propto\lambda_2^2$.

The nonzero value of E_0/L (disregarding this puzzling exponent) and the lack of any signal for a breakdown of parity show that the trajectory we are considering belongs to the phase with broken supersymmetry and unbroken Z_2 symmetry.

VII. CONCLUSION

In this paper, we investigated a class of two-dimensional $N=1$ Wess-Zumino models by nonperturbative lattice Hamiltonian techniques. The key property of the formulation is the exact preservation of a SUSY subalgebra at finite lattice spacing. Our main tools are numerical simulations using the Green function Monte Carlo algorithm; we also performed strong-coupling expansions.

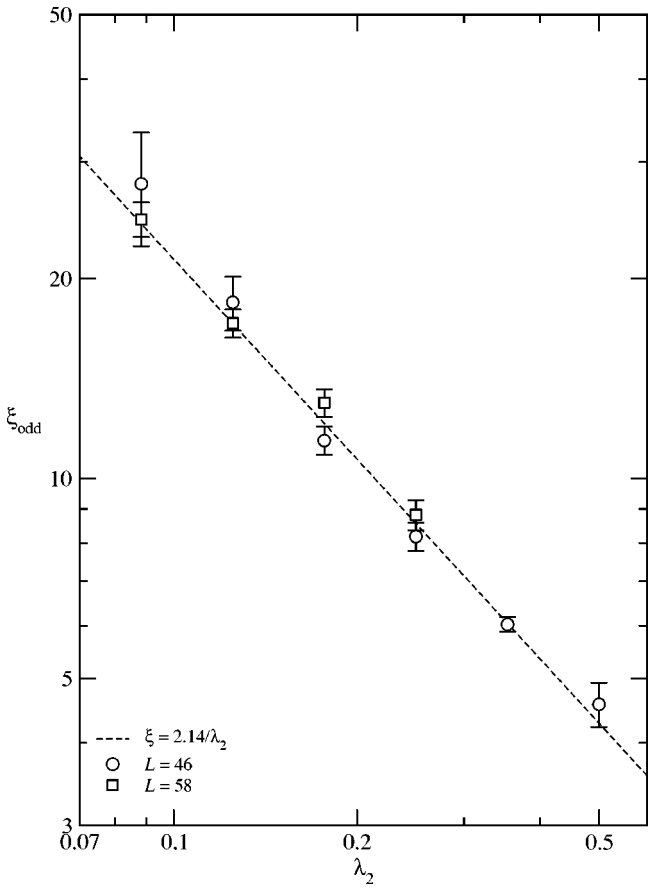

FIG. 16. The correlation length at odd distance ξ_{odd}. The dashed curve is the result of a scaling fit (with fixed exponent).

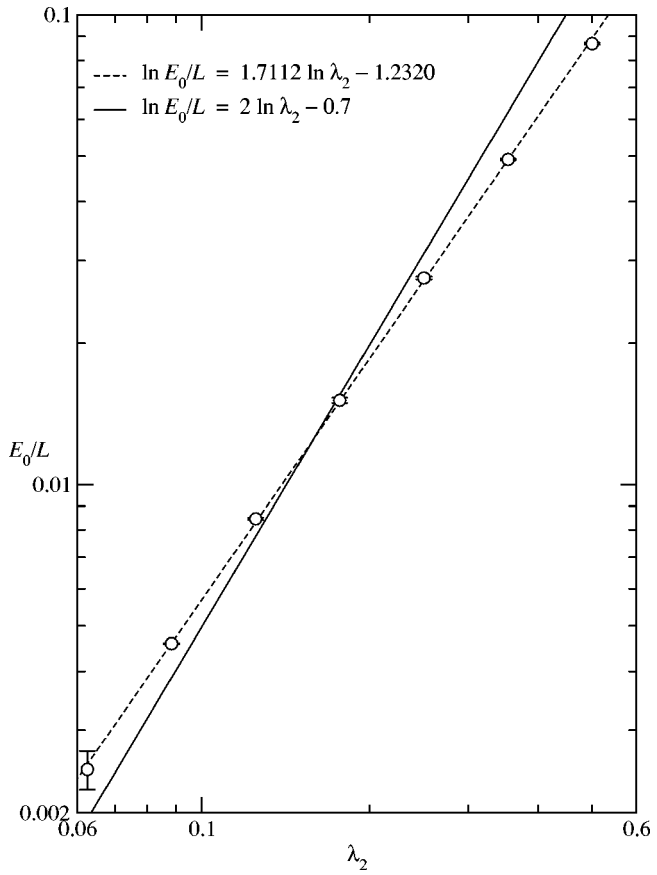

FIG. 17. The ground-state energy density E_0/L, extrapolated to $L\to\infty$ and $K\to\infty$. The dashed curve is the result of a two-parameter fit, while the solid curve shows the naïve scaling behavior.

All our results for the model with cubic prepotential indicate unbroken supersymmetry.

We studied dynamical supersymmetry breaking in the model with quadratic prepotential $V=\lambda_2\varphi^2+\lambda_0$, performing numerical simulations along a line of constant λ_2. We confirm the existence of two phases: a phase of broken SUSY and unbroken Z_2 at high λ_0 and a phase of unbroken SUSY and broken Z_2 at low λ_0, separated by a single phase transition.

We studied the approach to the continuum limit in the model with quadratic prepotential performing numerical simulations along a 1-loop RG trajectory in the phase of broken supersymmetry; we measured the correlation length of the bosonic field (in the odd-distance channel), which is found to scale with the expected exponent; on the other hand, the ground-state energy density scales with an exponent clearly different from the expected exponent.

In many instances, the simulation algorithm suffers from slow convergence in the number of walkers K.

ACKNOWLEDGMENTS

It is a pleasure to thank Camillo Imbimbo, Ken Konishi, Gianni Morchio, and Ettore Vicari for many helpful discussions and suggestions.

APPENDIX A: CHECK OF UNBROKEN SUSY FOR $V(\varphi)=\lambda_1\varphi+\lambda_0$

If the potential $V(\varphi)$ is a linear function of the field φ, then the ground state can be found explicitly. With a field translation we can set $\lambda_0=0$. The model Hamiltonian is H_B+H_F, where we recall that

$$H_B=\sum_{n=1}^{L}\left[\frac{1}{2}p_n^2+\frac{1}{2}\left(\frac{\varphi_{n+1}-\varphi_{n-1}}{2}+\lambda_2\varphi_n\right)^2\right], \tag{A1}$$

$$H_F=\sum_{n=1}^{L}\left[-\frac{1}{2}(\chi_n^\dagger\chi_{n+1}+\chi_{n+1}^\dagger\chi_n)+(-1)^n\lambda_2\chi_n^\dagger\chi_n\right]. \tag{A2}$$

Thus, in the bosonic sector, the Hamiltonian can be written

$$H_B=\frac{1}{2}\sum_n p_n^2+\frac{1}{2}\sum_{nm}\varphi_n V_{nm}^B\varphi_m, \tag{A3}$$

with

$$V_{nm}^B=\begin{cases}\lambda_2^2+1/4, & n=m \text{ and } n=1,L\\ \lambda_2^2+1/2, & n=m \text{ and } 1<n<L\\ -1/4, & |n-m|=2.\end{cases} \tag{A4}$$

In the fermionic sector, the Hamiltonian can be written in terms of canonical Fermi annihilation and creation operators as

$$H_F=\sum_{n,m} V^F_{nm} a^\dagger_n a_m \tag{A5}$$

with

$$V^F_{nm}=\begin{cases}(-1)^n\lambda_2, & n=m\\ \lambda_2^2+1/2, & n=m \text{ and } 1<n<L\\ -1/2, & |n-m|=1.\end{cases} \tag{A6}$$

If we denote by $\{(\omega^B_n)^2\}$ and $\{\omega^F_n\}$ the *sorted* eigenvalues of V^B and V^F, then we find that the ground state has actually zero energy,

$$E_0=\frac{1}{2}\sum_{n=1}^{L}\omega^B_n+\sum_{n=1}^{L/2}\omega^F_n=0. \tag{A7}$$

This can be proved in the spirit of SUSY without computing explicitly the eigenvalues. In fact, we can check that $(V^F)^2$ is the matrix V^B apart from a wrong sign in the diagonals $|n-m|=2$. This can be repaired by changing sign $\varphi\to-\varphi$ on the sites with $n \bmod 4=1,2$. Taking into account the particle-hole symmetry of H_F, we have thus proved that the spectra of $\sigma(V^F)$ and $\sigma(V^B)$ have the general form

$$\sigma(V^F)=\{-x_1,x_1,-x_2,x_2,\ldots\} \tag{A8}$$

$$\sigma(V^B)=\{x_1^2,x_1^2,x_2^2,x_2^2,\ldots\} \tag{A9}$$

with full cancellation between the lowest $L/2$ fermionic values and one half of the square root of the bosonic ones as in Eq. (A7).

APPENDIX B: STRONG-COUPLING EXPANSION OF $\langle\varphi_k\rangle$ AND $\langle\varphi_k\varphi_l\rangle_c$

1. $\langle\varphi_k\rangle$

Let us define

$$\overline{\varphi}=\langle\varphi\rangle_+=-\frac{\eta_0}{2\sqrt{2\varepsilon_0}}. \tag{B1}$$

The vacuum expectation value of the field φ is

$$\begin{aligned}\langle\Psi_0^{(1)}|\varphi_k|\Psi_0^{(1)}\rangle&=\overline{\varphi}(-1)^k\langle\Psi_0^{(1)}|(-1)^{n_k}|\Psi_0^{(1)}\rangle\\&=\overline{\varphi}(-1)^k(1-2\langle\Psi_0^{(1)}|n_k|\Psi_0^{(1)}\rangle).\end{aligned} \tag{B2}$$

The expectation value of the occupation number can be computed by going to the basis $\{a\}$ and is

$$\langle\Psi_0^{(1)}|n_k|\Psi_0^{(1)}\rangle=\sum_{p=1}^{L/2}(v_k^{(p)})^2. \tag{B3}$$

A straightforward calculation gives

$$\langle\Psi_0^{(1)}|n_k|\Psi_0^{(1)}\rangle=\frac{1}{2L}\left\{1+L+\frac{\cos\left[\frac{\pi}{2L}(2k(L+1)-1)\right]}{\sin\frac{\pi}{2L}(2k-1)}\right\}, \tag{B4}$$

and therefore

$$\langle\Psi_0^{(1)}|\varphi_k|\Psi_0^{(1)}\rangle=\frac{\eta_0}{2\sqrt{2\varepsilon_0}}(-1)^k\frac{1}{L}\left\{1+\frac{\cos\left[\frac{\pi}{2L}(2k(L+1)-1)\right]}{\sin\frac{\pi}{2L}(2k-1)}\right\}. \tag{B5}$$

It is interesting to consider the limit $L\to\infty$ of this expression after a rescaling $k\to xL$ where $0<x<1$. The result is

$$\langle\Psi_0^{(1)}|\varphi_{xL}|\Psi_0^{(1)}\rangle=\frac{\eta_0}{2\sqrt{2\varepsilon_0}}\left\{\frac{1}{L}[\pm1+\cot(\pi x)]+\frac{\pi}{2L^2}\frac{1}{\sin^2(\pi x)}+\mathcal{O}\left(\frac{1}{L^3}\right)\right\} \tag{B6}$$

where the sign is $+1$ for even $k=xL$ and -1 for odd k.

2. $\langle\varphi_k\varphi_l\rangle_c$

Let us denote briefly

$$\langle A\rangle\equiv\langle\Psi_0^{(1)}|A|\Psi_0^{(1)}\rangle, \tag{B7}$$

and

$$\langle AB\rangle_c=\langle AB\rangle-\langle A\rangle\langle B\rangle. \tag{B8}$$

The 2-point correlation is, for $k\neq l$,

$$\begin{aligned}\langle\varphi_k\varphi_l\rangle&=(\overline{\varphi})^2(-1)^{k+l}\langle(-1)^{n_k+n_l}\rangle\\&=(\overline{\varphi})^2(-1)^{k+l}(1-\langle n_k+n_k\rangle+4\langle n_k n_l\rangle).\end{aligned} \tag{B9}$$

Going to the $\{a\}$ basis, we immediately obtain

$$\langle n_k n_l\rangle_c=\sum_{1\le A\le L/2} v_k^A v_l^A\cdot\sum_{L/2+1\le B\le L} v_k^B v_l^B, \tag{B10}$$

and, for $k \neq l$,

$$\langle \varphi_k \varphi_l \rangle_c = 4(\overline{\varphi})^2 (-1)^{k+l} \langle n_k n_l \rangle_c . \tag{B11}$$

The two sums over eigenvalues can be evaluated analytically thanks to the simple form of the eigenvectors $v_l^{(p)}$. The explicit result is

$$\frac{L}{2} \sum_{p=1}^{L/2} v_n^{(p)} v_m^{(p)} = \frac{L}{4} \delta_{n,m} + \frac{1}{4} Z_{n,m}, \tag{B12}$$

$$\frac{L}{2} \sum_{p=1+L/2}^{L} v_n^{(p)} v_m^{(p)} = \frac{L}{4} \delta_{n,m} + \frac{1}{2}(-1)^{n+m} - \frac{1}{4} Z_{n,m}, \tag{B13}$$

where

$$Z_{n,m} = \begin{cases} n \text{ even}, \ m \text{ even}: & (-1)^{(n+m)/2} \left[1 + \cot \dfrac{\pi}{2L}(m+n-1) \right] \\ n \text{ even}, \ m \text{ odd}: & (-1)^{(n+m+1)/2} \left[1 + \cot \dfrac{\pi}{2L}(n-m) \right] \\ n \text{ odd}, \ m \text{ even}: & (-1)^{(n+m+1)/2} \left[1 + \cot \dfrac{\pi}{2L}(m-n) \right] \\ n \text{ odd}, \ m \text{ odd}: & (-1)^{(n+m)/2} \left[-1 + \cot \dfrac{\pi}{2L}(m+n-1) \right] \end{cases} \tag{B14}$$

that can be used to compute the connected correlation on a finite lattice.

It is interesting to note that the limit $L \to \infty$ can be taken without rescaling n and m. For instance, we have

$$\lim_{L\to\infty} \langle \Psi_0^{(1)} | \varphi_1 \varphi_n | \Psi_0^{(1)} \rangle_c = \frac{4(\overline{\varphi})^2}{\pi^2} (-1)^n \begin{cases} n \text{ even}: & \dfrac{1}{(n-1)^2} \\ n \text{ odd}: & \dfrac{1}{n^2}. \end{cases} \tag{B15}$$

APPENDIX C: SECOND-ORDER EXPANSION FOR E_0, EVEN q

The general formula for the second order contribution to the ground state energy is

$$E_2 = E_{2,1} + E_{2,2} \tag{C1}$$

$$E_{2,1} = \langle \Psi_0^{(1)} | H^{(4)} | \Psi_0^{(1)} \rangle \tag{C2}$$

$$E_{2,2} = \sum_{\Psi'} \frac{\langle \Psi_0^{(1)} | H^{(2)} | \Psi' \rangle \langle \Psi' | H^{(2)} | \Psi_0^{(1)} \rangle}{E_0 - E'}. \tag{C3}$$

The states $|\Psi'\rangle$ are excited states of the form

$$|\Psi'\rangle = \psi_{k_1}^{\sigma_1}(\varphi_1) \cdots \psi_{k_L}^{\sigma_L}(\varphi_L) |n_1, \ldots n_L\rangle$$

where $k_1 + \cdots k_L = \nu > 0$ (integer) and $\sigma_l = (-1)^{n_l + l}$. For such a state we have

$$E' = \sum_l \varepsilon_{k_l}.$$

A first important remark is that $H^{(2)}$ can be restricted to its $H_B^{(2)}$ part. In fact, the fermionic part of $H^{(2)}$ can be written as $H_{eff}^{(2)}$ plus terms that are only functions of the occupation numbers. These operators acting on $|\Psi_0^{(1)}\rangle$ give states that are orthogonal to the subspace of excited unperturbed states $|\Psi'\rangle$.

The first term in E_2 is simple and can be computed straightforwardly exploiting the fact that the expectation value of φ_l^2 over $|\Psi^{(1)}\rangle$ does not depend on l,

$$E_{2,1} = \frac{L-1}{4} \overline{\varphi^2} - \frac{1}{4} \sum_{l=1}^{L-2} \langle \Psi_0^{(1)} | \varphi_l \varphi_{l+2} | \Psi_0^{(1)} \rangle = \frac{L-1}{4} \overline{\varphi^2} - \frac{1}{4} (\overline{\varphi})^2 c_0(L) \tag{C4}$$

where

$$\overline{\varphi^2} = \int_{-\infty}^{\infty} \varphi^2 [\psi_0^{\pm}(\varphi)]^2 d\varphi$$

and

$$c_0(L) = \sum_{l=1}^{L-2} (1 - \langle n_l \rangle - \langle n_{l+2} \rangle + 4 \langle n_l n_{l+2} \rangle). \tag{C5}$$

About $E_{2,2}$, it can be computed by considering states with an excited single-site wave function in one or two distinct sites. Summing the two contributions we find

$$E_2=\frac{L-1}{4}\overline{\varphi^2}-\frac{1}{4}(\overline{\varphi})^2c_0(L)-\sum_{s>0}\frac{1}{\varepsilon_s-\varepsilon_0}\left(\frac{1}{2}(\Phi_s^{(1)})^2(V^{(0)})^2+c_1(L)\Phi_s^{(1)}V_s^{(1)}\overline{\varphi}V^{(0)}+c_2(L)(\overline{\varphi})^2(V_s^{(1)})^2\right)$$

$$-\sum_{s>0,\ t>0}\frac{1}{\varepsilon_s+\varepsilon_t-2\varepsilon_0}\left\{\frac{1}{4}(L-1)[(\Phi_s^{(1)})^2(V_t^{(1)})^2+(\Phi_t^{(1)})^2(V_s^{(1)})^2]+c_3(L)\Phi_s^{(1)}\Phi_t^{(1)}V_s^{(1)}V_t^{(1)}\right\}. \tag{C6}$$

The symbols appearing in the above equations are defined as follows:

$$V^{(0)}=\langle\psi_0^{\pm}|V(\varphi)|\psi_0^{\pm}\rangle=\sqrt{2\varepsilon_0}\,\eta_0 \tag{C7}$$

$$V_s^{(1)}=\frac{1}{\sqrt{2}}[\sqrt{\varepsilon_0}+(-1)^s\sqrt{\varepsilon_s}]\langle\psi_0^-|\psi_s^+\rangle, \tag{C8}$$

$$\Phi_s^{(1)}=-\frac{1}{\sqrt{2}}\frac{1}{\sqrt{\varepsilon_0}+(-1)^s\sqrt{\varepsilon_s}}\langle\psi_0^-|\psi_s^+\rangle. \tag{C9}$$

The functions $c_{0,1,2,3}(L)$ can be fitted with a few powers of L and the numerical result is

$$c_0(L)=L-1.495-\frac{2.610}{L}+\cdots \tag{C10}$$

$$c_1(L)=-0.540-\frac{1.698}{L}+\frac{1.787}{L^2}+\cdots \tag{C11}$$

$$c_2(L)=\frac{1}{2}L-0.540+\frac{0.301}{L}+\frac{1.788}{L^2}+\cdots \tag{C12}$$

$$c_3(L)=-\frac{2}{\pi^2}L-\frac{0.167}{L}+\cdots. \tag{C13}$$

The full expression for E_2 has thus the following simpler asymptotic expression:

$$\lim_{L\to\infty}\frac{E_2}{L}=\frac{1}{4}(\overline{\varphi^2}-\overline{\varphi}^2)-\frac{1}{2}(\overline{\varphi})^2\sum_{s>0}\frac{(V_s^{(1)})^2}{\varepsilon_s-\varepsilon_0}$$

$$-\sum_{s>0,t>0}\frac{1}{\varepsilon_s+\varepsilon_t-2\varepsilon_0}$$

$$\times\left\{\frac{1}{4}[(\Phi_s^{(1)})^2(V_t^{(1)})^2+(\Phi_t^{(1)})^2(V_s^{(1)})^2]\right.$$

$$\left.-\frac{2}{\pi^2}\Phi_s^{(1)}\Phi_t^{(1)}V_s^{(1)}V_t^{(1)}\right\}. \tag{C14}$$

As an example, we find for the model with $V(\varphi)=\varphi^2$,

$$E(\lambda^2,22)=0.2811-\frac{0.160}{\lambda^2}+\frac{0.0481}{\lambda^4}$$

and

$$E(\lambda^2,\infty)=0.2811-\frac{0.160}{\lambda^2}+\frac{0.0488}{\lambda^4}.$$

If we are interested in a comparison with an actual simulation, some trivial rescaling is necessary. For instance, in the case of a purely quadratic $V(\varphi)=\lambda_2\varphi^2$ we must compare the expansion and the results for $\lambda_2^{-2/3}E_0/L$ and identify $\lambda=\lambda_2^{1/3}$ as the strong-coupling expansion parameter.

APPENDIX D: FACTORIZED WAVE FUNCTION FOR THE FREE MODEL

In the free case $V\equiv 0$, with even L, we have

$$H^{(0)}=H_B+H_F, \tag{D1}$$

where ($\varphi_0=\varphi_{L+1}\equiv 0$, the same for fermions)

$$H_B=\sum_{n=1}^{L}\left\{\frac{1}{2}p_n^2+\frac{1}{8}(\varphi_{n+1}-\varphi_{n-1})^2\right\}, \tag{D2}$$

$$H_F=-\frac{1}{2}\sum_{n=1}^{L}(\chi_n^{\dagger}\chi_{n+1}+\chi_{n+1}^{\dagger}\chi_n). \tag{D3}$$

The two Hamiltonians H_B and H_F are decoupled and the ground state takes the factorized form

$$|\Psi^{(0)}\rangle=|\Psi_B^{(0)}\rangle\otimes|\Psi_F^{(0)}\rangle. \tag{D4}$$

We now determine $|\Psi_{B,F}^{(0)}\rangle$ separately, assuming $L \bmod 4=2$ in order to have a unique ground state in the decoupled $V\equiv 0$ model.

1. Bosonic sector

Let us write H_B in the form

$$H_B=\frac{1}{2}\sum_{n=1}^{L}p_n^2+\frac{1}{2}\sum_{n,m=1}^{L}V_{nm}\varphi_n\varphi_m. \tag{D5}$$

Let λ_k^2 be the eigenvalues of the $L\times L$ matrix V and let $z_n^{(k)}$ be the corresponding (real) eigenvectors satisfying

$$z^{(k)}\cdot z^{(l)}=\delta_{k,l}. \tag{D6}$$

The ground state is

$$\langle\varphi|\Psi_B^{(0)}\rangle=\exp\left(-\frac{1}{2}\sum_{n,m=1}^{L}R_{nm}\varphi_n\varphi_m\right), \tag{D7}$$

where

$$R_{nm}=\sum_{k=1}^{L}\lambda_k z_n^{(k)} z_m^{(k)}. \tag{D8}$$

The explicit form of λ_k is

$$\lambda_k=\sin\left(\frac{2i-1}{L+1}\frac{\pi}{2}\right),$$

$$i=\left\lfloor\frac{1}{2}(k+1)\right\rfloor \quad \left(i=1,\ldots,\frac{1}{2}L\right); \tag{D9}$$

the dimension of each eigenspace is 2. The ground state energy of H_B is

$$E_{0,B}=\sum_{k=1}^{L}\frac{1}{2}\lambda_k=\sum_{i=1}^{L/2}\sin\left(\frac{2i-1}{L+1}\frac{\pi}{2}\right). \tag{D10}$$

We adopt for the two orthogonal eigenvectors the choice

$$z_n^{(2i-1)}=\frac{2}{\sqrt{L+1}}\begin{cases}0 & (n \text{ even})\\ \sin\left(\dfrac{2i-1}{L+1}\dfrac{\pi}{2}(L-n+1)\right) & (n \text{ odd})\end{cases} \tag{D11}$$

$$z_n^{(2i)}=\frac{2}{\sqrt{L+1}}\begin{cases}\sin\left(\dfrac{2i-1}{L+1}\dfrac{\pi}{2}n\right) & (n \text{ even})\\ 0 & (n \text{ odd}).\end{cases} \tag{D12}$$

2. Fermionic sector

In the free case, the Hamiltonian in the fermionic sector is diagonalized by the orthogonal change of basis

$$\chi_x=\sqrt{\frac{2}{L+1}}\sum_{n=1}^{L}\sin\frac{n\pi x}{L+1}a_n, \tag{D13}$$

and takes the form

$$H_F=-\sum_{n=1}^{L}\cos\frac{n\pi}{L+1}a_n^\dagger a_n. \tag{D14}$$

Hence the one-fermion energies are

$$-\cos\frac{n\pi}{L+1}, \quad n=1,\ldots,L. \tag{D15}$$

The fermionic component of the (supersymmetric) ground state is

$$|\Psi_F^{(0)}\rangle=\prod_{n=1}^{L/2}a_n^\dagger|0\rangle; \tag{D16}$$

the ground state energy of H_F is

$$E_{0,F}=-\sum_{i=1}^{L/2}\cos\frac{n\pi}{L+1}; \tag{D17}$$

we can easily check that

$$E_{0,F}=-E_{0,B}=\frac{1}{2}\left(1-\frac{1}{\sin\dfrac{\pi}{2(L+1)}}\right), \tag{D18}$$

and therefore $E_0=E_{0,B}+E_{0,F}=0$.

[1] P. Langacker, *in Proceedings of the PASCOS90 Symposium*, edited by P. Nath and S. Reucroft (World Scientific, Singapore 1990); J. Ellis, S. Kelley, and D. Nanopoulos, Phys. Lett. B **260**, 131 (1991); U. Amaldi, W. de Boer, and H. Furstenau, *ibid.* **260**, 447 (1991); P. Langacker and M. Luo, Phys. Rev. D **44**, 817 (1991); C. Giunti, C.W. Kim, and U.W. Lee, Mod. Phys. Lett. A **6**, 1745 (1991).

[2] E. Witten, *Quest for Unification*, Lectures given at the 10th International Conference on Supersymmetry and Unification of Fundamental Interactions (SUSY02), Hamburg, Germany, 2002, hep-ph/0207124.

[3] S. Weinberg, Phys. Rev. D **13**, 974 (1976); **19**, 1277 (1979); L. Susskind, *ibid.* **20**, 2619 (1979); G. 't Hooft, in *Recent Developments in Gauge Theories*, Proceedings of the NATO Advanced Summer Institute, Cargese, 1979, edited by G. 't Hooft *et al.* (Plenum, New York, 1980).

[4] M. Beccaria, M. Campostrini, and A. Feo, *Adaptive Optimization of Wave Functions for Lattice Field Models*, contributed to ECT* Collaboration Meeting on Quantum Monte Carlo: Recent Advances and Common Problems in Condensed Matter and Field Theory, Trento, Italy, 2001, hep-lat/0109005; M. Beccaria, M. Campostrini, and A. Feo, Nucl. Phys. B (Proc. Suppl.) **106**, 944 (2002); **119**, 891 (2003); hep-lat/0309054.

[5] S. Catterall, J. High Energy Phys. **05**, 038 (2003); S. Catterall and S. Karamov, Phys. Rev. D **68**, 014503 (2003).

[6] K. Wilson, Phys. Rev. D **10**, 2445 (1974).

[7] J. Kogut and L.I. Susskind, Phys. Rev. D **11**, 395 (1975); J. Kogut, Rev. Mod. Phys. **51**, 659 (1979).

[8] M. Harada and S. Pinsky, Phys. Lett. B **567**, 277 (2003).

[9] D.M. Ceperley and M.H. Kalos, in *Monte Carlo Methods in Statistical Physics*, edited by K. Binder (Springer-Verlag, Heidelberg, 1992).

[10] I. Montvay and G. Münster, *Quantum Fields on a Lattice* (Cambridge University Press, Cambridge, England, 1994).

[11] A. Feo, Nucl. Phys. B (Proc. Suppl.) **119**, 198 (2003).

[12] E.Y. Loh, J.E. Gubernatis, R.T. Scalettar, S.R. White, D.J. Scalapino, and R.L. Sugar, Phys. Rev. B **41**, 9301 (1990).

[13] S. Coleman, Phys. Rev. D **11**, 2088 (1975).

[14] S. Mandelstam, Phys. Rev. D **11**, 3026 (1975).

[15] W. Von der Linden, Phys. Rep. **220**, 53 (1992). For an interesting complete solution of the sign problem in a class of models in 2+1 and 3+1 dimensions, see S. Chandrasekharan and

J. Osborn, Springer Proc. Phys. **86**, 28 (2000).
[16] E. Witten and D. Olive, Phys. Lett. **78B**, 97 (1978).
[17] S. Elitzur, E. Rabinovici, and A. Schwimmer, Phys. Lett. **119B**, 165 (1982).
[18] J. Ranft and A. Schiller, Phys. Lett. **138B**, 166 (1984).
[19] S. Elitzur and A. Schwimmer, Nucl. Phys. **B226**, 109 (1983).
[20] A. Schiller and J. Ranft, J. Phys. G **12**, 935 (1986).
[21] E. Witten, Nucl. Phys. **B188**, 513 (1981); F. Cooper, A. Khare, and U. Sukhatme, Phys. Rep. **251**, 267 (1995).
[22] B.R. Johnson, J. Chem. Phys. **67**, 4086 (1977).
[23] E. Witten, Nucl. Phys. **B202**, 253 (1982).
[24] M. Reed and B. Simon, *Methods of Modern Mathematical Physics, Vol. IV*: *Analysis of Operators* (Academic Press, New York, 1978).
[25] L. Alvarez-Gaume, D.Z. Freedman, and M.T. Grisaru (unpublished).
[26] S.A. Chin, Proceedings of the 1988 Symposium on Lattice Field Theory, Batavia, IL, 1988 [Nucl. Phys. B (Proc. Suppl.) **9**, 498 (1989)].
[27] J.H. Hetherington, Phys. Rev. A **30**, 2713 (1984).
[28] N. Trivedi and D.M. Ceperley, Phys. Rev. B **41**, 4552 (1990).
[29] M. Beccaria, Eur. Phys. J. C **13**, 357 (2000); Phys. Rev. D **61**, 114503 (2000); **62**, 034510 (2000); M. Beccaria and A. Moro, *ibid.* **64**, 077502 (2001).
[30] K. Binder, Z. Phys. B: Condens. Matter **43**, 119 (1981).
[31] A. Pelissetto and E. Vicari, Phys. Rep. **368**, 549 (2002).